PERGAMON

Deep-Sea Research II 47 (2000) 1387–1422

DEEP-SEA RESEARCH
PART II

Microbial food web structure in the Arabian Sea: a US JGOFS study

David L. Garrison[a,*], Marcia M. Gowing[a], Margaret P. Hughes[a], Lisa Campbell[b], David A. Caron[c], Mark R. Dennett[d], Alexi Shalapyonok[d], Robert J. Olson[d], Michael R. Landry[e], Susan L. Brown[e], Hong-Bin Liu[f], Farooq Azam[g], Grieg F. Steward[h], Hugh W. Ducklow[i], David C. Smith[j]

[a]*Institute of Marine Sciences, University of California, Santa Cruz, CA 95064, USA*
[b]*Department of Oceanography, Texas A&M University, College Station, TX 77843-3146, USA*
[c]*Department of Biological Sciences, University of South Carolina, 3616 Trousdale Parkway, AHF 309, Los Angeles, CA 90089-0371, USA*
[d]*Biology Department, Woods Hole Oceanographic Institution, Woods Hole, MA 02543, USA*
[e]*Department of Oceanography, University of Hawaii, 1000 Pope Rd., Honolulu, HI 96822, USA*
[f]*Marine Sciences Institute, The University of Texas at Austin, 750 Channel View Drive, Port Aransas, TX 78373, USA*
[g]*Scripps Institution of Oceanography, University of California, San Diego, CA 92093, USA*
[h]*Monterey Bay Aquarium Research Institute, P.O. Box 628, Moss Landing, CA 95039, USA*
[i]*The College of William and Mary, School of Marine Science; Box 1346, Gloucester Point, VA 23062, USA*
[j]*Graduate School of Oceanography, University of Rhode Island, Narragansett, RI 02882-1197, USA*

Received 4 May 1999; received in revised form 16 September 1999; accepted 17 September 1999

Abstract

One of the main objectives of the Joint Global Ocean Flux Studies (JGOFS) program is to develop an understanding of the factors controlling organic carbon production in the ocean and the time-varying vertical flux of carbon from surface waters (US JGOFS (1990) US JGOFS Planning Report Number 11; Sarmiento and Armstrong (1997) US JGOFS Synthesis and Modeling Project Implementation Plan). A considerable amount of evidence suggests that carbon cycling and the potential for exporting carbon from ocean systems is a function of food web structure. As part of the US JGOFS Arabian Sea Studies, the biomass of planktonic organisms, ranging from heterotrophic bacteria through microplankton-sized organisms, was estimated using a variety of methods including flow cytometry and microscopy. This is a first attempt to combine biomass data from a number of sources, evaluate the structure of the food

* Corresponding author. National Science Foundation, Division of Ocean Sciences, Biological Oceanography Program, Room 725, 4201 Wilson Blvd., Arlington, VA 22230, USA. Interpretations and conclusions are those of the author and do not imply the endorsement of the National Science Foundation.

0967-0645/00/$ - see front matter
PII: S0967-0645(99)00148-4

web, examine changes in food web structure in relation to seasonal or spatial features of the study area, and look for indications of how changing structure affects carbon-cycling processes.

Biomass in the upper 100 m of the water column ranged from approximately 1.5 to > 5.2 gC m^{-2}. Heterotrophic bacteria (Hbac) made up from 16 and 44% of the biomass; autotrophs comprised 43–64%; and the remainder was made up of nano- and microheterotrophs. Autotrophs and nano- and microheterotrophs showed a general pattern of higher values at coastal stations, with the lowest values offshore. Heterotrophic bacteria (Hbac) showed no significant spatial variations. The Spring Intermonsoon and early NE Monsoon were dominated by autotrophic picoplankton, *Prochlorococcus* and *Synechococcus*. The late NE Monsoon and late SW Monsoon periods showed an increase in the larger size fractions of the primary producers. At several stations during the SW Monsoon, autotrophic microplankton, primarily diatoms and *Phaeocystis* colonies, predominated. Increases in the size of autotrophs were also reflected in increasing sizes of nano- and microheterorophs. The biomass estimates based on cytometry and microscopy are consistent with measurement of pigments, POC and PON. Changes in community structure were assessed using the percent similarity index (PSI) in conjunction with multidimensional scaling (MDS) or single-linkage clustering analysis to show how assemblages differed among cruises and stations. Station clustering reflected environmental heterogeneity, and many of the conspicuous changes could be associated with changes in temperature, salinity and nutrient concentrations. Despite inherent problems in combining data from a variety of sources, the present community biomass estimates were well constrained by bulk measurements such as Chl *a*, POC and PON, and by comparisons with other quantitative and qualitative studies.

The most striking correlation between food web structure and carbon cycling was the dominance of large phytoplankton, primarily diatoms, and the seasonal maxima of mass flux during the SW Monsoon. High nutrient conditions associated with upwelling during the SW Monsoon would explain the predominance of diatoms during this season. The sinking of large, ungrazed diatom cells is one possible explanation for the flux observations, but may not be consistent with the observation of concurrent increases in larger microzooplankton consumers (heterotrophic dinoflagellates and ciliates) and mesozooplankton during this season. Food-web structure during the early NE Monsoon and Intermonsoons suggests carbon cycling by the microbial community predominated.

1. Introduction

The pelagic food web is comprised of a diversity of organisms varying over several orders of magnitude in size and differing in taxonomic affinities and trophic functions (e.g., Sieburth et al., 1978). Many of the smaller planktonic organisms, such as bacteria, picoplanktonic autotrophs and phagotrophic protists, were unknown or largely overlooked until relatively recently (e.g., Azam et al., 1983; Sherr and Sherr, 1984; Porter et al., 1985). Nonetheless, this assemblage, collectively known as the "microbial food web", is now recognized as ubiquitous and abundant in ocean environments (e.g., Garrison and Gowing, 1993; Buck et al., 1996; Table 5 in Garrison et al., 1998) with integral roles in system tropho-dynamics and biogeochemical transformations (Capriulo, 1990; Stoecker and Capuzzo, 1990; Caron et al., 1990; Caron, 1991; Gifford, 1991).

Assessing the structure and biomass composition of the pelagic food web has been one of the enduring research activities of plankton ecologists. Progress has largely

followed technical improvements in detecting and enumerating progressively smaller organisms (e.g., Fuhrman and McManus, 1984; Glover et al., 1986; Chisholm et al., 1988), as well as quantifying the abundance of organisms too rare to be adequately sampled in bottles or too delicate to be collected with nets (e.g., Gowing and Garrison, 1992). For the microbial community, epifluorescence microscopy (Booth, 1993; Sherr et al., 1993, Verity and Sieracki, 1993) and flow cytometry (Olson et al., 1990,1993; Button and Robison, 1993) techniques have been critical in allowing routine quantitative descriptions of, at least, the functional groups comprising the pelagic food web (e.g., see citations in Table 5 in Garrison et al., 1998).

The focus on accurate descriptions of the food web composition is driven by more than discovery or technology. It has long been recognized, for instance, that food web structure can profoundly affect ecosystem characteristics such as fish yield (Ryther, 1969), carbon flux, (Azam et al., 1983; Michaels and Silver, 1988; Peinert et al., 1989; Legendre and LeFevre, 1995; Legendre and Rassoulzadegan, 1996), and nutrient regeneration (Caron, 1991). Moreover, understanding of the underlying structure of food webs and the factors that cause them to develop in different ways is essential for developing and testing the predictive ecosystem and global-scale biogeochemical models that are ultimately desired by the JGOFS Program (e.g., Armstrong, 1994; Sarmiento and Armstrong, 1997).

The US JGOFS Arabian Sea Process Study was conducted to examine spatial and temporal variability in food web structure in a dynamic pelagic system (US JGOFS, 1990; Smith et al., 1991,1998a). Distributions and abundances of individual component populations have been reported previously (picoplankton: Campbell et al., 1998; Brown et al., 1999; Riemann et al., 1999; Ducklow et al., 2000a,b; nano- and microplankton: Garrison et al., 1998; Dennett et al., 1999; Caron and Dennett, 1999). Here we present the first combined effort to provide a comprehensive estimate of biomass structure and to evaluate spatial and temporal patterns in community structure.

2. Materials and methods

As part of the US JGOFS Arabian Sea Process Study, plankton community structure was investigated during four different phases of the monsoon cycle of 1995 (Table 1). Data were analyzed from seven stations (Fig. 1) for which we had reasonably complete data sets from all, or most, cruises. These included six stations (S1, S2, S4, S7, S11 and S15) along the southern transect extending from the upwelling-influenced coastal environment to the oligotrophic open ocean (Olson, 1991; Smith et al., 1998a; Garrison et al., 1998), and one offshore station (N7) on the northern transect.

Samples for this analysis were collected at four to six depths in the upper 100 m of the water column with 10-l Niskin bottles on a CTD rosette. The microbial assemblage was analyzed by dividing it into different size fractions and trophic groups that were enumerated separately using appropriate methodology (Table 2).

The specific methodology used to determine biomass and abundance of organisms has been reported in a number of recent papers (Campbell et al., 1998; Ducklow et al.,

Table 1
Cruise dates, hydrographic season, and summary of hydrographic conditions in the upper water column for stations on South transect, S1–S15. Mean and (range) of values are shown for all data. Temperature, salinity, and total nitrogen ($NO_3 + NO_2 + NH_4$) were averages from depths within the upper 20 m (data courtesy of J. Morrison et al.). Mixed layer depths ($mld_{0.125}$) were estimated as the depth where density changed by 0.125 kg m^{-3} from a near surface reference value as calculated and reported by W. Gardner and J. Gundersen. Chlorophyll *a* and primary production data courtesy of R. Barber and J. Marra. Chlorophyll values are averages within the upper 25 m. Primary production data are integrated data for the water column based on 24 h in situ incubations. All data and documentation are available from the JGOFS Arabian Sea data base (http://www1.whoi.edu/jgofs.html).

Cruise Dates Season	TN043 8 Jan.–4 Feb. NE Monsoon	TN045 14 Mar.–10 April Spring Intermonsoon	TN050 17 Aug.–15 Sept. Late SW Monsoon	TN054 28 Nov.–27 Dec. Early NE Monsoon
Temperature (°C)	25.4 (24.4–27.2)	26.9 (25.1–29.1)	26.0 (19.7–28.36)	27.0 (25.8–28.2)
Salinity (psu)	36.33 (36.10–36.55)	36.31 (35.23–36.69)	36.22 (35.63–36.614	36.47 (35.85–36.81)
Total nitrogen (μ moles)	2.27 (0.04–4.96)	0.25 (0.02–2.03)	5.83 (0.03–22.1)	0.79 (0.01–3.6)
N : Si	0.87 (0.01–2.2)	0.16 (0.01–1.1 1)	2.8 (0.02–18.0)	0.26 (0.00–2.1)
Mixed layer depth (m)	72 (68–76)	30 (10–70)	54 (24–100)	63 (50–82)
Chl *a* (μg l^{-1})	0.36 (0.05–0.95)	0.34 (0.02–0.93)	0.67 (0.01–1.72)	0.38 (0.12–0.88)
Primary production (g C m^{-2} day^{-1})	1.1 (0.6–1.4)	1.0 (0.7–1.3)	1.0 (0.6–1.8)	1.0 (0.7–1.4)

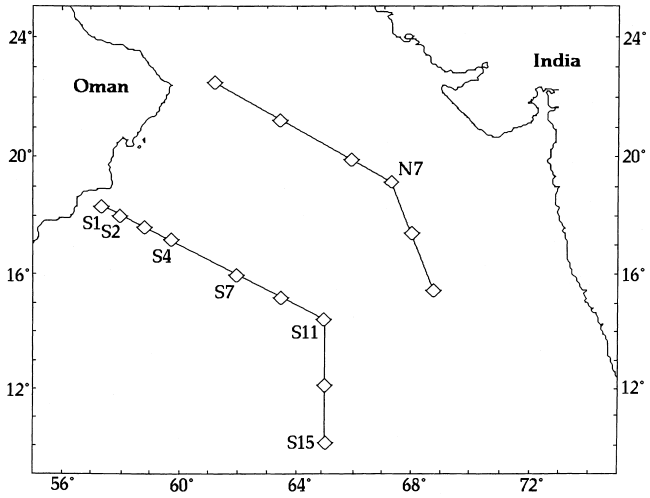

Fig. 1. JGOFS Stations in the northern Arabian Sea. Stations indicated were analyzed for this study, except that station S1 was not analyzed for the final of four cruises (TN054).

2000a,b; Garrison et al., 1998; Dennett et al., 1999). Here, these methods are briefly presented and discussed only as needed to explain the present synthesis of data.

2.1. Picoplankton

Picoplankton, including heterotrophic bacteria (Hbac), *Prochlorococcus* spp. (Pro), *Synechococcus* spp. (Syn), and phototrophic eukaryotes (Peuk), were counted using flow cytometry as described by Campbell et al. (1994,1998).

Cell carbon values for autotrophic picoplankton were determined as summarized in Table 2. Conversion values for Pro and Syn were based on recent calibrations by Shalapyonok et al. (2000) from cultures raised under natural light conditions. For picoeukaryotes, samples from TN054 were sized using forward angle light scattering (FALS) to determine a size-frequency distribution, which we assumed was similar for all cruises. Approximately 69% (range 27–88%) of the eukaryotic cells were > 2.0 μm. These counts were removed from cytometer data to avoid overlap with microscopical counts of autotrophic nanoplankton. The remaining cells (31%) were assumed to comprise the picoeukaryotes. Cell volumes were calculated assuming a 1.5 μm-diameter spherical shape, and cell volume-to-carbon conversions based on a modified Strathmann equation for non-diatom phytoplankton (Eppley et al., 1970) were used to estimate carbon.

Flow cytometer counts were used for heterotrophic bacteria (Hbac) estimates for all cruises for consistency (no filter counts were available for TN050). A regression (Model II) of all paired estimates of Hbac by cytometer and epifluorescence microscopy produced the regression: cytometer (bacteria cells l^{-1}) $= 1.044 \times$ epifluorescence (cells l^{-1}) $- 0.870 \times 10^8$ (cells l^{-1}); ($R^2 = 0.689$, $n = 421$), with a regression coefficient

Table 2
Overview of methods and conversion factors used to estimate carbon biomass for different components of the microbial food web. Values taken from the literature are shown with source citations. Details of methods used for nano- and microplankton and interpretations of distributions are presented in Dennett et al. (1999) and Garrison et al. (1998). Specific descriptions of some methods are in the text. CYT: flow cytometry; EFM: epifluorescence microscopy; LM: light microscopy. In formulae below V = cell volume (μm^{-3})

Size fraction group	Methods for enumeration	Conversions used for biomass pg C Cell^{-1}	fg C μm^{-3}	Remarks and citations
Picoplankton (0.2– ~ 2.0 μm)				
Heterotrophic picoplankton	CYT EFM	0.011	380	Average from TN045 and TN049 data. See text
Autotrophic picoplankton				
Prochlorococcus	CYT	0.032/0.072	235	Mixed layer populations/Below mixed layer
Synechococcus	CYT	0.101/0. 152	235	Mixed layer populations/Below mixed layer
Picoeukaryotes	CYT	1.011		See text
Nanoplankton (2–20 μm)				
Autotrophic nanoplankton	EFM		183	TN043, TN045; Caron et al., 1995.
		$\log_{10}$ C = 0.94($\log_{10}$ V) − 0.60	210[a]	TN050, TN054 (Eppley et al., 1970; Garrison et al., 1998)
Heterotrophic nanoplankton	EFM		183	TN043, TN045 (Caron et al., 1995)
		$\log_{10}$ C = 0.94($\log_{10}$ V) − 0.60	(209/211)[a]	TN050, TN054 (Garrison et al., 1998)
Microautotrophs (> 20 μm)				
Other algae	EFM		183	TN043, TN045 (Caron et al., 1995)
		$\log_{10}$ C = 0.94($\log_{10}$ V) − 0.60		TN050, TN054
Diatoms	LM/EFM	$\log_{10}$ C = 0.76($\log_{10}$ V) − 0.352		All Cruises (Eppley et al., 1970)
Dinoflagellates	LM/EFM		140	TN043, TN045 (Stoecker et al., 1994)
		$\log_{10}$ C = 0.94($\log_{10}$ V) − 0.60	(183/165)[a]	TN050, TN054 (Eppley et al., 1970)
Microheterotrophs (> 20 μm)				
Dinoflagellates	LM/EFM		140	TN043, TN045
		$\log_{10}$ C = 0.94($\log_{10}$ V) − 0.60	(164/160)[a]	TN050, TN054
Non-loricate ciliates	LM		140	TN043, TN045
			160–190	TN050, TN054 (Putt and Stoecker, 1989)
Tintinnids	LM		53	TN043, TN045 (Verity and Langdon, 1984)
			160–190	TN050, TN054 (Putt and Stoecker, 1989)

[a]Average value of carbon per volume (fg C μm^{-3}) for cruises TN050 and TN054 data for comparisons with those used for TN043 and TN045 (see Dennett et al., 1999)

not different from 1.0. The cell sizes of (Hbac) were determined by epifluorescence microscopy for cruises TN045 and TN049 (Ducklow et al., 2000a). Mean bacterial volumes were measured on every cell counted in every sample and cell volume calculated using the algorithm of Baldwin and Bankston (1988) (mean = 0.029 μm^3; range = 0.019–0.056 μm^3; $N = 421$, upper 0–200 m), and carbon content was determined by assuming 380 fgC μm^{-3} (Lee and Fuhrman, 1987). An average value of 11 fg C $cell^{-1}$ for these two cruises was used to estimate bacterial biomass from abundance for all cruises.

2.2. Nanoplankton

Both autotrophic and heterotrophic nanoplankton were concentrated on filters and counted by epifluorescence microscopy as described by Garrison et al. (1998) and Dennett et al. (1999). Preservation and staining methods varied among the cruises (see Garrison et al., 1998; Dennett et al., 1999). During TN043 and TN045 (Dennett et al., 1999), water samples were preserved at a final concentration of 1% formalin (made in natural, filtered seawater) and stored at 4°C. Samples were prepared for enumeration by epifluorescence microscopy within 24 h of preservation by staining with DAPI at a final concentration of 50 $\mu g\ ml^{-1}$ (Caron, 1983; Sherr et al., 1993). For TN050 and TN054 (Garrison et al., 1998), replicate samples were stained separately with the fluorochromes DAPI (Coleman, 1980) and proflavine (Haas, 1982) + DAPI (e.g., Verity and Sieracki, 1993). Glutaraldehyde and the fluorochromes were added near the end of the filtration when approximately 10 ml remained in the filter chimney. The final concentration of glutaraldehyde was $\sim 0.5\%$.

2.3. Microplankton

Water samples were preserved with Lugol's Iodine solution or buffered paraformaldehyde for analysis of the robust microplankton including diatoms, silicoflagellates, thecate and some athecate dinoflagellates and ciliates. These samples were counted by inverted microscopy (see Garrison et al., 1998; Dennett et al., 1999). For both filter-collected and whole water samples, carbon estimates were derived by measuring cell dimensions, calculating cell volumes and applying carbon to volume conversion factors (Table 2).

2.4. Size fractions

Biomass in conventional size fractions (i.e., pico-, nano- and microplankton) was calculated as follows: picoplankton sizes were confirmed by FALS analysis of cytometer data, and the fraction comprising pico-eukaryotes was distinguished from the wider range of eukaryotic autotrophs detected by the cytometer as described in Campbell et al. (1994,1998). For TN043 and TN045, biomass data are separated into nano- and microplankton size fractions Dennett et al. (1999), but taxonomic groups within the autotrophic nanoplankton (Anan) and heterotrophic nanoplankton (Hnan) were not differentiated. For TN050 and TN054 microbial groups within the

nanoplankton were distinguished by taxon and cell volume. To have a consistent grouping of categories that would allow an analysis among all cruises, size fractions of nano- and microplankton were grouped using cell volume ranges of > 4.2 to 4190 μm^3 and > 4190 μm^3, respectively, to separate cells into nano- and microplankton and data recombined in a manner consistent with that used for TN043 and TN045.

2.5. Analysis of the microbial assemblage

We used community analysis procedures similar to those outlined by Field et al. (1982) to examine the similarity of assemblage composition between stations and cruises and to assess which biomass components were responsible for the variations. Biomass was classified within the 12 size and taxonomic components (Table 3). Similarities were calculated between paired stations as Percent Similarity Index (PSI):

$$\mathrm{PSI}(\mathrm{Sample}_{a,b}) = \sum \mathrm{Minimum}[\mathrm{Group}_i(\%\mathrm{Sample}_a, \%\mathrm{Sample}_b)]$$

where, $i =$ (groups $1, 2 \ldots, 12$) in a comparison of the similarity between samples a and b. The resulting station-by-station similarity matrix was analyzed using multi-dimensional scaling (MDS) and single-linkage cluster analysis (see Field et al., 1982 for a more complete discussion of these procedures). We did not use transformed biomass data, as suggested by Field et al. (1992), to avoid the bias of giving unwarranted weighting to ciliate biomass. Tintinnid data from TN050 and TN054, in particular, sometimes were based on samples with low cell counts and thus have wide confidence limits. Analyses and clustering were performed on both transformed and untransformed data. Both produced similar station clustering patterns but the latter proved easier to interpret.

3. Results

3.1. Community Composition

The overall ranges of abundance and biomass of microbial groups are summarized in Table 3. Depth-integrated biomass over the upper 100 m of the water column (or 85 m at S1 where bottom depth did not extend to 100 m) ranged from approximately 1.5 to > 5.2 g Cm^{-2} (Table 4). Overall, autotrophs made up 43–64% of the biomass; Hbac accounted for 16–44%, and nano- and microheterotrophic protists comprised the remaining portion (Table 4). Biomass estimates for total microbial biota, autotrophic, nano- and microheterotrophic, and bacterial biomass were not significantly different among the four cruises (Duncan multiple-range test, $\alpha < 0.05$; SAS Institute Inc., 1989). Among stations and within cruises, total autotrophic and nano- and microheterotroph biomass estimates were generally higher for coastal stations (S1 and S2) and lower at the offshore stations (N7–S15), but usually only the extreme values could be distinguished statistically (see Table 5). Heterotrophic bacteria showed no statistically significant differences among stations. Based on analysis of discrete-depth

Table 3
Range of abundance and biomass for different microbial groups over the four cruises analyzed ($0.0 \leqslant 0.05$)

Cruise	Biomass			Abundance		
Size fraction		μg C l^{-1}			cell l^{-1}	
Microbial group	Mean	Min	Max	Mean	Min	Max
TN043						
Picoplankton						
Heterotrophic bacteria	8.0	0.2	11.5	7.3E + 08	1.8E + 07	1.0E + 09
Prochlorococcus	1.0	0.0	7.2	3.0E + 07	3.3E + 04	2.3E + 08
Synechococcus	3.7	0.1	112.9	3.7E + 07	7.9E + 04	1.3E + 08
Picoeukaryotes	0.6	0.0	1.8	1.3E + 06	9.9E + 03	3.9E + 06
Nanoplankton						
Autotrophic nanoplankton	5.6	0.2	18.1	7.6E + 05	2.7E + 04	2.9E + 06
Heterotrophic nanoplankton	4.3	0.9	12.3	3.7E + 05	1.3E + 05	9.8E + 05
Microplankton						
Dinoflagellates	2.1	0.0	27.6	5.6E + 02	0.0E + 00	2.2E + 03
Diatoms	3.4	0.0	27.6	2.7E + 04	2.2E + 02	2.0E + 05
Autotrophic flagellates	0.3	0.0	7.5	9.9E + 01	0.0E + 00	9.6E + 02
Heterotrophic dinoflagellates	2.3	0.0	32.4	5.5E + 02	0.0E + 00	2.6E + 03
Non-loricate ciliates	0.5	0.0	2.4	5.0E + 02	0.0E + 00	2.6E + 03
Tintinnids	0.0	0.0	0.1	4.7E + 01	2.4E + 00	1.3E + 02
TN045						
Picoplankton						
Heterotrophic bacteria	10.2	2.8	31.8	9.2E + 08	2.6E + 08	2.9E + 09
Prochlorococcus	8.6	0.0	47.2	1.7E + 08	3.3E + 04	7.0E + 08
Synechococcus	3.6	0.0	33.0	2.8E + 07	1.6E + 04	2.2E + 08
Picoeukaryotes	0.4	0.0	2.3	9.7E + 05	1.0E + 04	5.2E + 06
Nanoplankton						
Autotrophic nanoplankton	4.8	0.1	15.2	5.3E + 05	1.1E + 04	1.4E + 06
Heterotrophic nanoplankton	4.6	0.7	12.1	3.0E + 05	1.3E + 05	8.0E + 05
Microplankton						
Dinoflagellates	1.4	0.0	5.2	1.4E + 03	2.4E + 01	5.1E + 03
Diatoms	0.8	0.0	8.8	4.7E + 03	1.1E + 02	6.0E + 04
Autotrophic flagellates	0.1	0.0	0.9	6.9E + 01	0.0E + 00	4.1E + 02
Heterotrophic dinoflagellates	0.6	0.0	2.2	5.9E + 02	1.0E + 01	2.2E + 03
Non-loricate ciliates	0.4	0.0	2.6	3.2E + 02	2.1E + 01	1.3E + 03
Tintinnids	0.0	0.0	0.2	5.4E + 01	1.2E + 00	2.5E + 02
TN050						
Picoplankton						
Heterotrophic bacteria	11.4	3.8	23.5	1.0E + 09	3.4E + 08	2.1E + 09
Prochlorococcus	1.6	0.0	9.10	4.4E + 07	3.6E + 04	2.8E + 08
Synechococcus	3.0	0.1	9.5	2.8E + 07	3.7E + 04	9.4E + 07
Picoeukaryotes	0.9	0.0	5.8	2.0E + 06	1.1E + 04	1.3E + 07
Nanoplankton						
Autotrophic nanoplankton	4.6	0.1	36.3	4.2E + 05	3.2E + 03	2.0E + 06
Heterotrophic nanoplankton	2.9	0.5	10.1	5.4E + 05	3.5E + 04	2.2E + 06

Table 3 (*continued*)

Cruise	Biomass			Abundance		
Size fraction		μg C l^{-1}			cell l^{-1}	
Microbial group	Mean	Min	Max	Mean	Min	Max
Microplankton						
Dinoflagellates	0.7	0.0	2.9	4.2E + 05	4.2E + 05	4.2E + 05
Diatoms	5.5	0.0	36.8	3.7E + 03	1.0E + 01	2.6E + 04
Autotrophic flagellates[a]	3.8	0.1	18.7	6.6E + 05	8.2E + 03	2.8E + 06
Heterotrophic dinoflagellates	1.0	0.1	4.6	2.6E + 02	3.0E + 01	1.0E + 03
Non-loricate ciliates	0.9	0.1	4.4	3.0E + 02	3.0E + 01	1.2E + 03
Tintinnids	0.2	0.0	1.5	8.0E + 01	1.0E + 01	3.0E + 02
TN054						
Picoplankton						
Heterotrophic bacteria	11.3	1.5	34.7	1.0E + 09	1.4E + 08	3.2E + 09
Prochlorococcus	2.8	0.2	10.2	8.4E + 07	3.2E + 05	3.2E + 08
Synechococcus	9.8	0.1	54.2	9.7E + 07	3.5E + 04	5.4E + 08
Picoeukaryotes	0.9	0.0	3.3	2.1E + 06	1.1E + 04	7.4E + 06
Nanoplankton						
Autotrophic nanoplankton	2.3	0.1	9.8	3.0E + 05	9.0E + 03	8.0E + 05
Heterotrophic nanoplankton	1.7	0.1	9.5	1.8E + 05	9.2E + 03	7.9E + 05
Microplankton						
Dinoflagellates	0.5	0.0	1.9	1.7E + 02	1.0E + 01	1.1E + 03
Diatoms	0.5	0.0	2.3	6.0E + 02	1.0E + 01	2.6E + 03
Autotrophic flagellates	0.0	0.0	0.0	0.0E + 00	0.0E + 00	0.0E + 00
Heterotrophic dinoflagellates	1.3	0.1	6.1	5.0E + 02	6.0E + 01	1.9E + 03
Non-loricate ciliates	1.1	0.0	5.2	2.6E + 02	2.4E + 01	1.1E + 03
Tintinnids	0.3	0.0	2.3	8.0E + 01	1.0E + 01	3.4E + 02

[a]Mostly *Phaeocystis* non-motile cells in disrupted colonies; see methods and Garrison et al. (1998).

samples, biomass estimates for Hbac, autotrophs, and other heterotrophs were negatively correlated with depth (Spearman; $R = -0.55, -0.70, -0.59$; $N = 240$, 172, 171; $P < 0.01$ for the three groups, respectively).

3.2. Seasonal and spatial distributions

The composition of the microbial community varied among stations and cruises (Table 5). To identify seasonal (between cruises) and spatial (between station) differences for each of the 12 groups of the microbial community, we examined both the depth-integrated (Table 5) and discrete-depth data (not shown) using the Duncan multiple-range test (SAS Institute Inc., 1989). Trends were considered significant at $\alpha < 0.05$. Pro biomass was higher during TN045 than during other cruises, and Syn biomass was higher during TN054. Autotrophic microflagellate (Aflg) biomass was highest during TN050, and non-loricate ciliate (Cil) biomass was higher for TN050

Table 4
Integrated biomass (g C m^{-2}) of major groups of microbial organisms. Data integrated from surface to 100 m at all stations except S1, where bottom depth and depth of integration was 85 meters. % composition is the percent of the total biota biomass. n.d.; no POC, PON data for TN050

Integrated biomass parameters g C m^{-2}	TN043			TN045			TN050			TN054		
	Mean	min	max	Mean	min	max	Mean	min	max	Mean	min	max
Heterotrophic bacteria	0.74	0.51	0.99	0.96	0.72	1.49	1.04	0.60	1.73	0.84	0.52	1.74
	26%	16%	36%	29%	23%	33%	32%	20%	44%	26%	17%	36%
Autotrophs	1.40	0.72	2.83	1.88	1.23	2.65	1.77	1.06	2.89	1.24	0.76	1.85
	50%	45	58%	55%	45%	61%	53%	43%	64%	50%	44%	57%
Heterotrophs	1.36	0.83	2.34	1.48	1.07	2.10	1.53	1.08	2.40	1.27	0.89	2.30
	50%	42%	54%	44%	38%	55%	47%	36%	57%	50%	43%	56%
Total Microbial biomass	2.76	1.55	5.17	3.36	2.61	4.75	3.30	2.43	5.29	2.50	1.73	4.15
POC	4.81	3.07	7.25	5.36	3.43	7.28	n.d.	n.d.	n.d.	3.35	2.44	5.08
Microbial biomass/POC	57%	44%	71%	64%	37%	76%				51%	43%	64%
C : N (From POC, PON)	5.5	5.2	5.9	6.0	5.6	6.6	7.5	6.1	10.1	3.5	2.9	4.1
(From population estimates)	5.2	5.0	5.7	5.0	4.9	5.1	5.2	4.9	5.7	5.0	4.8	5.1
Chl *a* (mg m^{-2})	34	22	48	31	18	41	55	23	124	41	24	61
C : Chl *a*	36	19	48	63	38	81	38	23	53	32	19	52

Table 5
Integrated carbon biomass (g C m^{-2}) for microbial groups in the upper water column (85 m at station S1 and 100 m for all other stations). Cruises outlined had significantly higher biomass based on Duncan multiple-range test ($\alpha \leqslant 0.05$). For analysis of temporal and spatial variations, biomass values for S1 were normalized to 100 m

Cruise	Station	Hbac	Pro	Syn	Peuk	Anan	Hnan	Aflg	Adin	Diat	Hdin	Ncil	Tin
TN043	S1	0.82	0.01	0.15	0.04	0.83	0.61	0.12	0.74	0.95	0.87	0.04	0.01
	S2	0.72	0.02	0.24	0.03	0.60	0.64	0.02	0.13	0.39	0.15	0.06	0.01
	S4	0.84	0.05	0.28	0.06	0.29	0.21	0.01	0.06	0.21	0.06	0.03	0.01
	S7	0.69	0.04	0.61	0.10	0.54	0.31	0.00	0.03	0.14	0.02	0.06	0.00
	S11	0.99	0.12	0.55	0.06	0.41	0.35	0.02	0.16	0.03	0.10	0.05	0.00
	S15	0.64	0.49	0.12	0.04	0.34	0.35	0.00	0.02	0.06	0.01	0.03	0.00
	N7	0.51	0.01	0.25	0.04	0.29	0.21	0.01	0.06	0.07	0.07	0.05	0.00
TN045	S1	0.94	1.51	0.31	0.05	0.58	0.57	0.01	0.07	0.00	0.03	0.04	0.00
	S2	0.99	0.94	0.18	0.03	0.51	0.46	0.00	0.25	0.21	0.11	0.07	0.01
	S4	1.49	1.15	0.73	0.06	0.52	0.54	0.02	0.11	0.06	0.05	0.03	0.00
	S7	0.87	0.63	0.41	0.03	0.26	0.40	0.01	0.08	0.10	0.05	0.03	0.00
	S11	0.81	0.78	0.09	0.04	0.38	0.25	0.00	0.16	0.02	0.06	0.02	0.00
	S15	0.72	0.92	0.03	0.04	0.50	0.26	0.01	0.16	0.02	0.06	0.02	0.00
	N7	0.90	0.06	0.48	0.04	0.40	0.48	0.00	0.12	0.13	0.06	0.03	0.00
TN050	S1	0.61	0.04	0.08	0.11	1.01	0.36	0.18	0.05	0.49	0.06	0.05	0.01
	S2	0.92	0.02	0.12	0.18	0.46	0.48	0.24	0.11	1.16	0.10	0.14	0.01
	S4	1.09	0.00	0.11	0.04	0.19	0.15	0.06	0.06	0.63	0.08	0.09	0.01
	S7	1.19	0.01	0.32	0.04	0.44	0.36	1.01	0.04	0.28	0.08	0.07	0.06
	S11	1.73	0.01	0.30	0.04	0.36	0.26	1.29	0.11	0.81	0.25	0.12	0.04
	S15	0.92	0.59	0.39	0.03	0.10	0.22	0.10	0.01	0.00	0.03	0.02	0.01
	N7	0.79	0.50	0.37	0.04	0.17	0.18	0.06	0.07	0.10	0.08	0.10	0.00
TN054	S2	1.74	0.36	1.59	0.08	0.36	0.17	0.00	0.06	0.11	0.20	0.11	0.07
	S4	0.52	0.38	0.69	0.09	0.22	0.12	0.00	0.05	0.05	0.12	0.14	0.00
	S7	0.77	0.35	1.04	0.12	0.19	0.19	0.00	0.06	0.03	0.14	0.15	0.03
	S11	0.85	0.24	0.72	0.08	0.18	0.15	0.00	0.02	0.03	0.17	0.07	0.01
	S15	0.53	0.74	0.18	0.05	0.24	0.20	0.00	0.03	0.01	0.08	0.07	0.06
	N7	0.65	0.11	0.39	0.04	0.14	0.11	0.00	0.01	0.06	0.07	0.13	0.01

and TN054 than for TN043 and TN045 (Table 5). Discrete-depth analysis produced similar results for these comparisons (see Table 3 for range of values within cruises). Other patterns were suggested but not as clearly indicated. For example, diatom (Diat) biomass was high during TN043 and TN050 and not statistically different between these cruises, and lower during TN045 and TN054 (also not statistically different from one another). However, total diatom biomass during TN043 could not be distinguished from diatom biomass values during TN045 (see Table 5). Analysis of discrete-depth samples, however, showed average biomass concentrations of diatoms with TN050 > TN043 > TN045, TN054.

Similar to the results of between-cruises comparisons, biomass variations among stations within cruises showed few significant trends for total integrated stocks, but

patterns could be identified when discrete depths were analyzed. Syn biomass was higher at S1 than other stations, and Pro was highest at station S15. Many of the groups showed distributions suggesting an onshore-to-offshore decrease in biomass, but as was the case for integrated biomass, sometimes the data were only significantly higher for S1 > S15, with intermediate stations along the onshore-offshore transect showing higher biomass values (e.g., see Table 5).

3.3. Size structure

Aggregation of groups into conventional size fractions (i.e., pico-, nano-, and micro-) and trophic modes (i.e., autotrophs and heterotrophs) revealed some conspicuous patterns. During the Spring Intermonsoon (TN045: Fig. 2b) and the early NE Monsoon (TN054: Fig. 2d), picoplankton dominated the autotrophic assemblages at all stations, and their biomass was significantly higher than during cruises TN050 and TN043. In contrast, during the well-developed NE (TN043: Fig. 2a) and SW Monsoons (TN050: Fig. 2c), nano- and microautotrophs were relatively more important with respect to biomass. Autotrophic microplankton biomass was significantly higher during the SW Monsoon (TN050), dominating total autotrophic biomass at stations S2–S11 (Fig. 2c). Diatoms contributed to the increase in the larger fractions during both TN043 and TN050 (Table 5), and colonies of *Phaeocystis* were particularly abundant at stations S7 and S11 during TN050. Overall, variations in the size fractions of heterotrophs followed those shown by autotrophs. That is, autotrophic microplankton biomass was positively correlated with heterotrophic microplankton biomass (Spearman; $R = 0.44$; $P < 0.05$), and heterotrophic nanoplankton was positively correlated with autotrophic nanoplankton ($R = 0.083$; $P < 0.05$).

3.4. Biomass parameters

Carbon-to-chlorophyll *a* ratios (C : Chl *a*, where C was determined from autotrophic biomass estimates) from depth-integrated data (Table 4) averaged 36, 63, 38, and 32 for TN043, TN045, TN050, and TN054, respectively. Analysis of discrete-depth samples showed significant negative relationships with depth (Spearman; $R = -0.33$; $N = 119$; $P < 0.01$). These data were grouped subsequently, with samples above the $\mathrm{mld}_{0.125}$ or 1% light levels considered "surface layer" samples versus those occurring below the mixed layer or the 1% light level considered "deep" samples (see Table 1 for explanation of mixed layer determination). A multiple-range test (Duncan, $\alpha < 0.05$) showed higher C : Chl *a* ratios in surface-layer samples from TN045, but no significant differences were found between deep and shallow samples for other cruises, or among mean ratios for these cruises. Fig. 3 shows the scatter of data around the slopes derived from cruise averages of C : Chl a ratios for discrete-depth samples.

The biota in the pico- to microplankton size ranges accounted for 37–76% of particulate organic carbon (POC) (Biota C/POC; Table 4). There was a wider range of values from discrete depth samples (12–250%), but estimated biota biomass exceeded measured POC in only 4 of 115 data pairs. Mean values of Biota C/POC were not

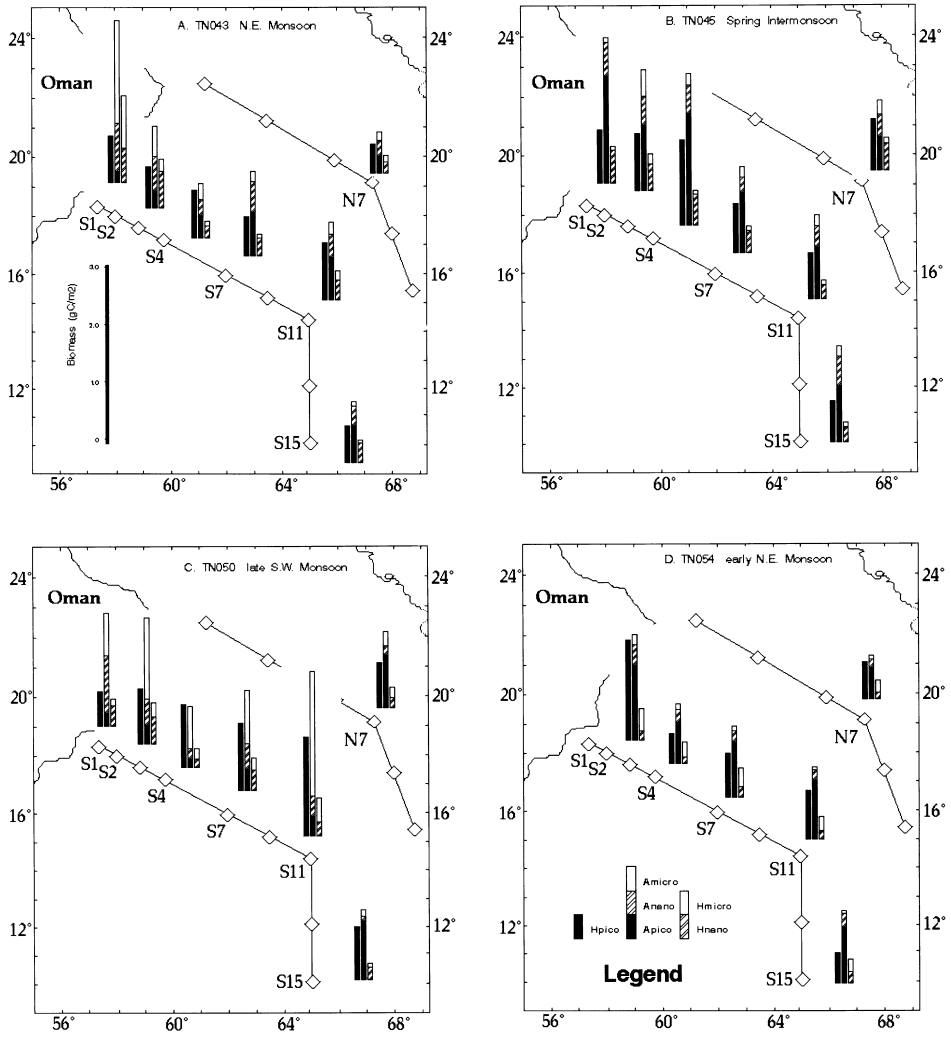

Fig. 2. Biomass within different size fractions for each station. Integration of data is the same as in Tables 4 and 5. Picoplankton (< 2 μm). Nanoplankton (2–20 μm). Microplankton (> 20 μm).

significantly different among the three cruises for which POC measurements were available (TN043, TN045, and TN054) (Duncan multiple-range test, $\alpha < 0.05$). With substantial overlap in confidence ranges among individual stations, no spatial patterns were evident within cruises. The percent carbon accounted for by organisms was unrelated to depth in the upper 100 m (Pearson correlation; $R = -0.11$, $P > 0.20$, $N = 115$).

From depth-integrated data (Table 4), we also calculated the stocks of PON associated with organisms by assuming a C : N ratio (atoms) of 4.0 for Hbac (Lee and

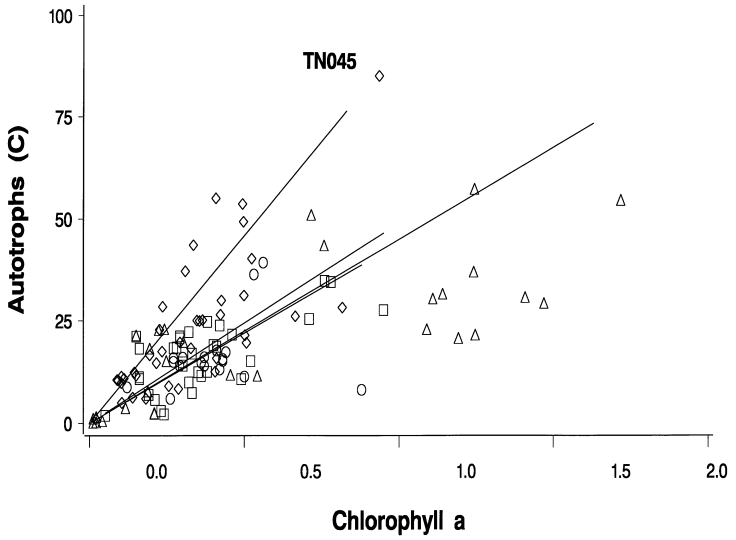

Fig. 3. Autotrophic C : Chl. *a* ratios for discrete-depth samples. TN043: Squares. TN045: Diamonds. TN050: Triangles. TN045: Circles. Slopes for each cruise were calculated from average ratios of surface samples (TN045; C : Chl $a = 92$), or all samples on the other cruises where surface and deep samples were not found to have significantly different C:Chl a ratios. Average ratios for TN043, TN050, and TN054 were 49, 45, and 44, respectively; these were not significantly different. The slope for TN045 is the only one specifically identified in the figure.

Fuhrman, 1987; Caron, 1991; Caron et al., 1995), 5.0 for Pro (L. Campbell, unpublished data) and Syn (Verity et al., 1992), 6.6 for all autotrophic eukaryotes, and 5.8 for heterotrophic eukaryotes (Caron et al., 1990). The difference between POC and PON and the corresponding C and N associated with organisms produced an unidentified fraction (detritus and some unaccounted-for biota such as large protozooplankton, metazoa, and so forth) with C : N ratios of 6.1 (5.6–7.7), 12.3 (6.7–18.8), and 2.7 (2.2–3.3) for cruises TN043, TN045, and TN054, respectively (no data for TN050).

3.5. Spatial and temporal variations of assemblages

The pattern of station clustering for all cruises, based on the multiple dimensional scaling (MDS) analysis of the station-by-station percent similarity matrix (PSI), is shown in Fig. 4. The general similarity of stations within cruises is evident, with the exception that stations S15 and N7 appear as outliers from their cruise-station clusters. A differing pattern of spatial variability for each cruise is also suggested in Fig. 4, and this impression is supported by the relatively high variability and lower average similarity among stations during TN043 and TN050 versus the relatively low spatial variability and higher average similarities during TN045 and TN054 (Table 6, upper).

Overall, heterotrophic bacteria (Hbac) were responsible for 33–42% of the similarity relationship among stations within each cruise (Table 6, lower), and this

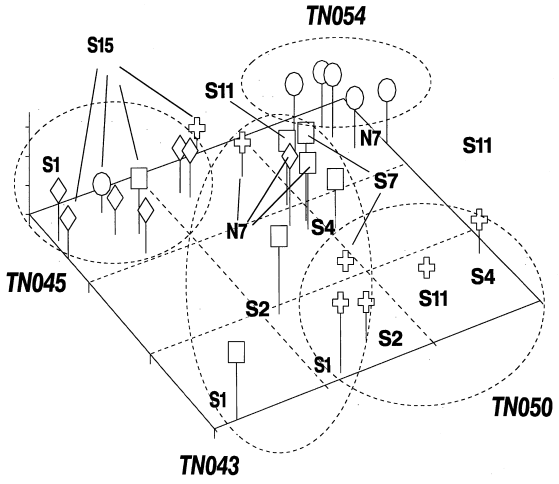

Fig. 4. Similarity plot produced by multi-dimensional scaling (MDS) using 3-dimensional representation. Cruises: TN043 (squares); TN045 (diamonds); TN050 (crosses); TN054 (circles). Axes (not labeled) are arbitrary distance; the distances between stations on the MDS plot are proportional to the dissimilarity (1-PSI) between assemblages. Dashed ovals were added to illustrate cruise clusters of stations.

Table 6
Results from similarity analyses among stations for each cruise. Similarity among stations is the average value of the PSI value calculated from comparisons among all station combinations within each cruise. Group contribution was determined as the average of Minimum [$Group_i$(%$Sample_a$,%$Sample_b$)]/PSI between comparisons of adjacent stations (see Materials and Methods for calculation of PSI)

Similarity among stations (%)		TN043	TN045	TN050	TN054
	Mean	73	81	68	80
	Range	53–89	63–93	45–85	61–90
Ranking of group contribution to similarity		Tint 0.00	Tint 0.00	Tint 0.00	Aflg 0.00
		Aflg 0.00	Aflg 0.00	Adin 0.02	Tint 0.01
		Pro 0.01	Ncil 0.01	Peuk 0.02	Adin 0.01
		Ncil 0.02	Peuk 0.01	Pro 0.03	Diat 0.03
		Peuk 0.02	Diat 0.02	Hdin 0.03	Peuk 0.03
		Hdin 0.03	Hdin 0.02	Ncil 0.03	Ncil 0.05
		Adin 0.03	Adin 0.04	Aflg 0.07	Hdin 0.051
		Diat 0.06	Syn 0.09	Syn 0.08	Hnan 0.07
		Syn 0.12	Hnan 0.15	Diat 0.10	Pro 0.08
		Hnan 0.15	Pro 0.15	Hnan 0.10	Anan 0.10
		Anan 0.20	Anan 0.16	Anan 0.10	Syn 0.24
		Hbac 0.33	Hbac 0.36	Hbac 0.42	Hbac 0.35

relationship did not change markedly over the cruises. In contrast, other groups and the order of their relative importance (in contributing to biomass) varied among cruises. For example, Anan were second in importance to Hbac for all cruises except for TN054 where variations in Syn became more important. Microplankton groups,

in general, accounted for less of the variation in biomass structure, except during TN050, where Diat were of similar importance to Anan and Hnan with respect to variations in biomass structure.

The specific patterns of community variability (shown in Table 5 and Fig. 4) were clearer when individual cruises were analyzed separately for similarity using single-linkage clustering analysis. During the NE Monsoon (TN043), there was a relatively high level of similarity among the stations (average PSI = 73%; Table 6), but coastal station, S1, and offshore station, S15, joined the clusters at lower levels of similarity (cluster data not shown, but see positions of stations in Fig. 4 relative to other stations in station-cluster for TN043). Over all the stations, Hbac, Anan, Hnan and Syn accounted for most of the similarity relationship (Table 6), but the importance of specific groups varied with station (Table 5). For example, Anan, Hbac and Diat were primarily responsible for the similarity among stations S1, S2, and S4; in comparisons among S4, S7 and S11, Syn replaced Diat in accounting for variability; and in a comparison of the assemblage at S11 versus S15, Hnan, Syn, and Pro accounted for significant amounts of the variability in addition to Hbac and Anan. The community structure at S11 differed from that at S15 due to the relative biomass changes between Syn (higher at S11) and Pro (higher at S15; Table 5). The single northern transect station, N7, was most similar to S7 or S11 (Fig. 4). As was the case with stations S7 and S11, Hbac, Syn, Anan, and Hnan were the biomass dominants at N7.

The pattern of community variability during the Spring Intermonsoon (TN045) differed from that shown in the preceding season (TN043). The average similarity was higher and the range lower (Table 6). Stations formed a smaller similarity cluster (Fig. 4), and similarity between adjacent stations was high (range 82–94%; Table 6). The major difference during TN045 was the high biomass of Pro at many stations. Northern transect station N7 clustered well outside the station-cluster group for TN045 (Fig. 4). An examination of the clustering of N7 with other stations indicated that structure at N7 was most like that at S7. The difference between N7 and S7 (as well as the other southern stations) was the low biomass of Pro at N7 (Table 5).

The highest variability observed during the study was during the late SW Monsoon season (TN050). Similar to TN043, diatoms were important contributors to community structure at coastal stations, but during TN050 they were also important at offshore stations out to approximately S11 (Table 5). Although diatoms were still an important component of the biomass at stations S7 and S11, these stations formed a cluster that was distinct from S1, S2, and S4 because of *Phaeocystis* colonies (or disrupted colonies) present at stations S7 and S11 (Aflg in Table 5). In contrast, the picoautotrophs Pro or Syn were important at offshore stations S15 and N7 (Table 5). Also in contrast to the other cruises, Station N7 was more similar to the offshore station S15 than to any of the other stations (Fig. 4).

The early NE Monsoon (TN054) was characterized by relatively little spatial variability, except that offshore station S15 differed from the remaining stations nearer to shore (Fig. 4). Assemblages during this cruise were markedly dominated by picoplankton (Fig. 3d), with Hbac and Syn important components of the biomass at all stations (Table 5). Compared to other cruises, Hdino were also relatively important during TN054 (Tables 5 and 6). The marked change in structure between stations S11

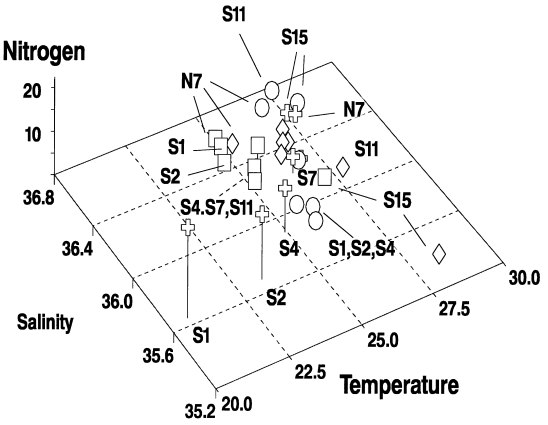

Fig. 5. Temperature, salinity vs. total nitrogen ($NO_3 + NO_2 + NH_4$). Values are averages for upper 20 meter samples at each station. Range of values is given in Table 1. TN043: Squares. TN045: Diamonds. TN050: Crosses. TN045: Circles.

and S15 was a result of the high biomass of Pro and a lower relative biomass of Syn at S15 (Table 5).

3.6. Hydrography and assemblages

We had expected that biomass accumulations would be related to physical and chemical characteristics of surface waters (Table 1) and would vary both temporally and spatially. The ranges of temperature, salinity, mixed layer depth, nutrient concentrations, productivity, and phytoplankton biomass (Chl *a*) showed considerable overlap among seasons and stations within cruises (Table 1; Fig. 5). Some of this variability could be associated with the patterns of similarity among stations (e.g., Fig. 4). During TN043, all stations except S15 fell within ranges of 24.60–25.78°C, 36.20–36.53‰, and 1.2–3.9 μM for temperature, salinity and total nitrogen, respectively. At station S15, in contrast, salinities were < 36.20‰, temperatures were > 27.0°C, and total inorganic nitrogen levels were low (0.04 μM). During TN045, total nitrogen concentrations were low at all stations (maximum 0.5 μM at N7), and stations S15, S11, and N7 showed a clustering of temperature and salinity characteristics that differed from other stations during this cruise (Fig. 5). TN050 was conducted near the end of the SW Monsoon, and upwelling along the coast was conspicuous during this season. A gradient, extending from the low temperatures, low salinities and higher nutrients of the upwelling-influenced coastal stations to the warmer, higher salinity and nutrient-depleted offshore waters was evident for stations S1–S11 (Fig. 5). Stations S15 and N7 were distinguished by temperatures > 27°C and low nutrients (Total N < 0.05 μM). TN054 was identified as the beginning of the NE Monsoon season for 1995–96 (Morrison et al., 1998). This period was characterized by low nutrient concentrations, increased temperatures and higher salinities relative to TN050, and a general deepening of the mixed layer (Table 2).

4. Discussion

4.1. Community composition

The primary objective of this study was to assess the time-varying biomass structure of the microbial assemblage during the US JGOFS Arabian Sea investigation and to examine how varying structure related to seasonal changes in carbon cycling processes. A robust quantitative estimate of the various components of the food web is the first requirements for such a synthesis.

By necessity, our analysis was restricted to four of seven US JGOFS cruises where microscopical studies were conducted. Nevertheless, data from three monsoon seasons and one intermonsoon period (Table 1) are representative of the extremes of seasonal differences for the region. Similarly, the southern transect (Stations S1–S15) covered environments varying from the upwelling-influenced coastal regions, across the axis of the Findlater Jet where the wind curl stress changes from positive to negative, and an oceanic region characterized by a deep mixed layer and relatively oligotrophic conditions (see Smith et al., 1998a).

There are uncertainties when combining data from different sources to determine the composition of microbial assemblages, including concerns about the accuracy and consistency of identifying and enumerating specific organisms, obtaining complementary data with differing techniques, and the choices of factors for converting cell counts and biovolume to carbon. The latter uncertainty is well-known (e.g., Choi and Stoecker, 1989; Putt and Stoecker, 1989; Verity et al., 1992; Stoecker et al., 1994; Dennett et al., 1999; Shalapyonok et al., 2000). Our approach was to use recently derived conversions where such exist (see Table 2). As a practical matter, it was not possible to analyze replicate samples for all data that needed to be combined (e.g. cytometry and microscopy) or compared (e.g., other biomass parameters such as Chl *a*, POC, and PON). Some data were combined from adjacent depths and from consecutive (or the nearest) casts at the same station where necessary to provide full data sets; no attempt has been made to assess this source of variability.

We used cytometer data for estimates of Hbac because these were the only data available for TN050. Whereas we observed a close correspondence between cytometer abundance data and epifluorescence counts for the data sets overall (a regression not significantly different from 1 – see Methods), individual cruises showed variations on the order of 20% (Ducklow et al., 2000a,b). There is also uncertainty in the biomass conversion used for this group. We used the conversion factor of 380 fg C μm^{-3} (Lee and Fuhrman, 1987) for cells ranging from 0.019 to 0.056 μm^3 (average = 0.029 μm^3; carbon $cell^{-1}$ = 11 fg). Lee and Fuhrman's (1987) conversion was based on larger cells (0.036–0.730 μm^3), and if their observed negative relationship between carbon per volume and cell volume is extrapolated to the generally smaller cells observed during this study, the biomass conversions of 11 fg C $cell^{-1}$ could be low by a factor of 2. Recent work by Fukuda et al. (1998) has demonstrated that no single conversion is satisfactory and that the carbon per cell may range from around 30 fg C $cell^{-1}$ in coastal waters to around 12 fg C $cell^{-1}$ for oceanic bacteria. Pomroy and Joint (1999) determined bacterial biomass in the same region of the Arabian Sea a year prior to the

US JOGFS study. They estimated cell carbon of 10.5 and 7.5 fg C cell^{-1} for the SW Monsoon (September) and intermonsoon (November–December), respectively. Our conversion factor of 11 fg C cell^{-1} seems reasonable when compared with the data from Fukuda et al. (1998) and Pomroy and Joint (1999). Because estimates for picoeukaryotes (Peuk) (discussed below) are conservative and because we have not accounted for larger protozoans and micro-metazoans (see Dennett et al., 1999), the lower estimate of Hbac may be more tenable if POC measurements are assumed to constrain estimates of the biota. However, based on Fukuda et al. (1998), it seems likely that bacteria may have been underestimated at coastal stations.

Reliable abundance estimates of autotrophic prokaryotes (Pro and Syn) by cytometry are possible because of the specific pigment signatures and light scattering properties of these forms (Olson et al., 1990), and these cells fall within a relatively narrow size range. However, a variety of values have been used for converting cell numbers to carbon; many are significantly higher than values used in the present study (e.g. Buck et al., 1996; Campbell et al., 1998; Tarran et al., 1999; Shalapyonok et al., 2000). In analyzing cytometry samples for other US JGOFS Arabian Sea cruises (TN049 and TN053, two cruises just prior to TN050 and TN054 analyzed here), Shalapyonok et al. (2000) found that carbon per cell for both Pro and Syn varied significantly between cells from within and below the mixed layer (Table 2); hence, these new values have been used in the present synthesis.

The quantification of picoeukaryotes by cytometry is more ambiguous than that for autotrophic prokaryotes because the pigment signatures of these forms are similar to those of larger eukaryotic algae. Moreover, in addition to true "picoplankton-sized cells", there is a relatively continuous size-spectrum for autotrophic eukaryotic cells detected by cytometry (Olson et al., 1990). For the four cruises analyzed here, we have attempted to restrict cytometry data for eukaryotes to cells $< 2\,\mu m$. Based on forward angle light scatter (FALS) analysis of a set of samples from TN054, we found that 31% of the cells enumerated as "picoeukaryotes" were $< 2\,\mu m$ (see Methods). By eliminating cells $> 2\,\mu m$ from the data set and assuming that this fraction was detected by epifluorescence microscopy, we may have underestimated cells in the 2–5 μm range. For discrete-depth samples from TN054 (24 depths), we found that cytometer estimates for cells in the $> 2\,\mu m$ range averaged 6.8×10^6 cells l^{-1} (range: 1.2×10^5 to 1.4×10^7). In contrast, estimates for microscopy counts for cells 2–5 μm (cell volumes: $4.9 \geqslant 49\ \mu m^{-3}$) averaged only 2.7×10^5 cells l^{-1} (range: 1.8×10^3 to 7.5×10^5). If we assume that cytometry counts also may include cells $> 5\,\mu m$, then the agreement would improve. Nevertheless, our analysis – based on only one cruise – suggests that microscopic estimates are conservative for the approximately 2–5 μm cell-size range relative to the cytometry estimates. It is not clear from our limited analysis which technique is the most accurate.

Biomass estimates of the nano- and microplankton were made using similar methods but by two different research teams (TN043 and TN045: Dennett et al., 1999; TN050 and TN054: Garrison et al., 1998), and with different biovolume-to-carbon conversion factors. For cruises TN043 and TN045, constant conversion factors were used for organisms other than diatoms. For cruises TN050 and TN054, some biomass estimates were based on a modified Strathmann equation, where carbon per volume

Table 7
A comparison of carbon biomass estimates using a constant volume-to-carbon conversion versus a volume-dependent conversion (a modified Strathmann expression). See Table 2 for the specific conversion factors. Estimates were calculated by each method for the same set of data for cruises TN050 and TN054, and the comparisons are expressed as (estimate using constant/estimate using Strathmann expression). *N*, mean, and standard deviation are shown.

	TN050			TN054		
	N	Mean	STD	*N*	Mean	STD
A. Nano						
nano	35	0.87	0.047	30	0.87	0.010
micro	32	0.89	0.025	30	0.87	0.001
A. Dino						
nano	38	0.82	0.023	30	0.81	0.020
micro	25	0.95	0.178	27	1.02	0.049
H. Nan						
	35	0.87	0.022	30	0.87	0.017
H. Dino						
nano	40	0.82	0.020	30	0.80	0.018
micro	38	1.00	0.102	30	1.03	0.053
Ciliates						
nano	39	0.87	0.006	30	0.88	0.000
micro	40	0.87	0.007	30	0.87	0.001

varies inversely with cell volume (Eppley et al., 1970). Based on average values for cell volume for TN050 and TN054 (Table 2), biomass estimates using the Strathmann relationship should be higher than estimates using the constant carbon : volume relationship, with the magnitude of the difference varying with cell size (nanoflagellates $\sim$ 18% higher and dinoflagellates ranging from 14 to 31% higher). Recalculations of the entire data sets from TN050 and TN054, however, showed relatively close agreement where different conversion factors were used (Table 7). Thus, the use of different volume-to-carbon conversions probably would have only a minor effect on differences observed in assemblages between cruises (TN043 and TN045) and (TN050 and TN054) (e.g., Table 5).

Assigning organisms to specific trophic categories has other potential errors. Mixotrophic protists were present in the nano- and microplankton size fractions (Porter, 1988; Sanders and Porter, 1988; Bockstahler and Coats, 1993; Stoecker et al., 1989; Putt, 1990; Caron and Swanberg, 1990), but they could not be rigorously quantified for any of the cruises (Garrison et al., 1998; Dennett et al., 1999).

Bulk estimates of biomass (Chl *a*, POC and PON) provide one means of constraining estimates of organism biomass from cytometry and microscopy. Ratios of C : Chl *a*, where C is determined by microscopy or direct measurement of carbon in unialgal cultures, range from approximately 10 to 130 for nutrient-replete cells grown at

a range of temperatures and light levels (Geider, 1987). The C : Chl a ratios we observed (Table 4, Fig. 3) were within ranges predicted for populations at 20–30°C. The significantly higher C : Chl *a* for TN045 (92) may be the result of stratification and lower nutrient availability (total nitrogen = 0.24 μm; Table 1 and see Morrison et al., 1998). Furthermore, Pro also predominated during this cruise. Shalapyonok et al. (2000) reported similar values (112 ± 29) for TN053 where, as was the case with TN045, prokaryotic picoplankton predominated. They attributed the high C : Chl *a* ratio to photoacclimation at higher light levels and increased stratification, as well as to the presence of prokaryotic forms with higher cellular carbon concentrations. The Shalapyonok et al. (2000) estimates for C : Chl *a* for the SW Monsoon period (TN049; 57 ± 29) were similar to those observed later in this season (TN050; mean = 45).

Larger protozoans (e.g., sarcodines) and micro-metazoans (naupliar larvae) were included in the analyses for TN043 and TN045 (Dennett et al., 1999) but were not in the present synthesis because similar data were not available for TN050 and TN054. Their inclusion would only raise the biomass estimate of living biota by 1–2% of POC (Table 4). In contrast, if higher values for bacterial carbon were used (20 vs. 11 fg C $cell^{-1}$) the average estimate of living biomass would increase as much as 20% (for TN054), and at some stations living biomass estimates would exceed POC estimates. Similarly, including higher estimates for picoeukaryotes also would increase the living biomass as a % of POC and raise C : Chl *a* ratios.

For the two cruises where the comparison could be made, there was good qualitative agreement of our clusters of stations based on microscopy and those from pigment analyses (Latasa and Bidigare, 1997). Both analyses identified the Pro-dominated stations along the southern transect during the Spring Intermonsoon (TN045; approximately stations S1–S7; Table 5; Fig. 1 in Latasa and Bidigare, 1997) as distinct from northern station, N7, where Pro was relatively unimportant. There was a more striking correspondence for the analyses during the SW Monsoon (TN050), where picoplankton-dominated offshore stations (S15 and N7) were clearly distinguished from Diat-dominated coastal stations (S1–S4; see Table 5). Stations S7 and S11 on the mid Southern transect also were distinguished from the others by high concentrations of *Phaeocystis* and (apparently) senescent diatoms (see Garrison et al., 1998; Latasa and Bidigare, 1997).

4.2. Spatial and temporal variations of assemblages

The seasonal and spatial dynamics of picoplankton (Campbell et al., 1998) and nano- and microplankton (Garrison et al., 1998; Dennett et al., 1999) for the four cruises used in our analysis have been described previously, so discussion here is limited to significant areas of agreement or where qualifications of previous conclusions are now indicated.

The changing monsoon seasons and local hydrography produce an environmental mosaic that apparently gives rise to differing planktonic assemblages. The extremes may be characterized by warm, nutrient-poor conditions where picoplankton, primarily Pro, predominate (S15 during most seasons) and during the Spring

intermonsoon (TN045) versus the relatively cold, nutrient-rich, and microplankton-dominated SW Monsoon season (TN050) (Fig. 5; Morrison et al., 1998).

Both NE and SW Monsoon seasons (TN043 and TN050) showed a response in community structure characterized by increases in the size of autotrophs and heterotrophs (Fig. 2a and c). In many cases the increase in the size spectrum of the autotrophs could be related to the increase in diatom abundance (Tables 5 and 6). This effect was more pronounced for the SW Monsoon (TN050) than for the NE Monsoon (TN043). During TN043, for example, diatoms and autotrophic nanoplankton predominated mostly at coastal stations (approximately S1–S4; Table 5), whereas during the SW Monsoon (TN050) larger autotrophs, and diatoms in particular, predominated out as far as station S11(Fig. 2c, Table 5). In contrast, cruises TN045 and TN054 were characterized by the prevalence of smaller forms (Fig. 2b and d; Table 5).

It seems likely that the differences we observed between early (TN054) and later (TN043) NE Monsoon periods relate to the seasonal development of the NE Monsoon hydrographic conditions. One of the distinctive features of the NE Monsoon is the deep convective mixing with surface cooling resulting both from decreasing solar insulation and from cooling winds from the Asian continent (Morrison et al., 1998). This cooling reaches its maximum during January and February, and the progression can clearly be seen in the time-series of satellite-derived sea surface temperature presented by Morrison et al. (1998); (their Fig. 3). Relative to TN043, conditions during TN054 were characterized by warmer sea-surface temperatures, shallower mixed layers, and lower nutrient concentrations (Table 1). Assemblages during TN054 were, however, similar to those described for TN053 by Shalapyonok et al. (2000), except that during TN053 Pro was relatively more important than Syn, sea surface temperatures were generally warmer, mixed layers were shallower, and nutrients were generally lower (Shalapyonok et al., 2000; Morrison et al., 1998). The assemblages we describe for TN054 are similar to those reported by Tarran et al. (1999) from the ARABESQUE studies in November and December, 1994 (further discussed below and see Fig. 6b). Thus, a change in the microbial assemblage during the development of the NE Monsoon may be a regular feature of the community succession.

4.3. Comparisons with other studies

Understanding if the structure of food webs varies spatially and temporally in a predictable manner is fundamental in ocean ecology. Comparisons among studies require a consistent and accurate assessment of food web components. An initial evaluation of the individual data set making up this compilation, primarily based on comparing results to studies elsewhere, has been reported by Campbell et al. (1998) and Liu et al. (1998) for picoplankton and Garrison et al. (1998) and Dennett et al. (1999) for nano- and microplankton. Whereas many of the recent major ocean studies have collected data on the various components of the food web (e.g., references cited above; Stelfox et al., 1999; Shalapyonok et al., 2000), relatively few have attempted a comprehensive synthesis of food web structure (however, see Buck et al., 1996).

The ARABESQUE studies (Burkill, 1999) are of particular interest because they were conducted in the same region of the Northern Arabian Sea a year prior to the US JGOFS effort and thus provide an opportunity to assess interannual variability. Abundance and biomass estimates from the separate components of the microbial

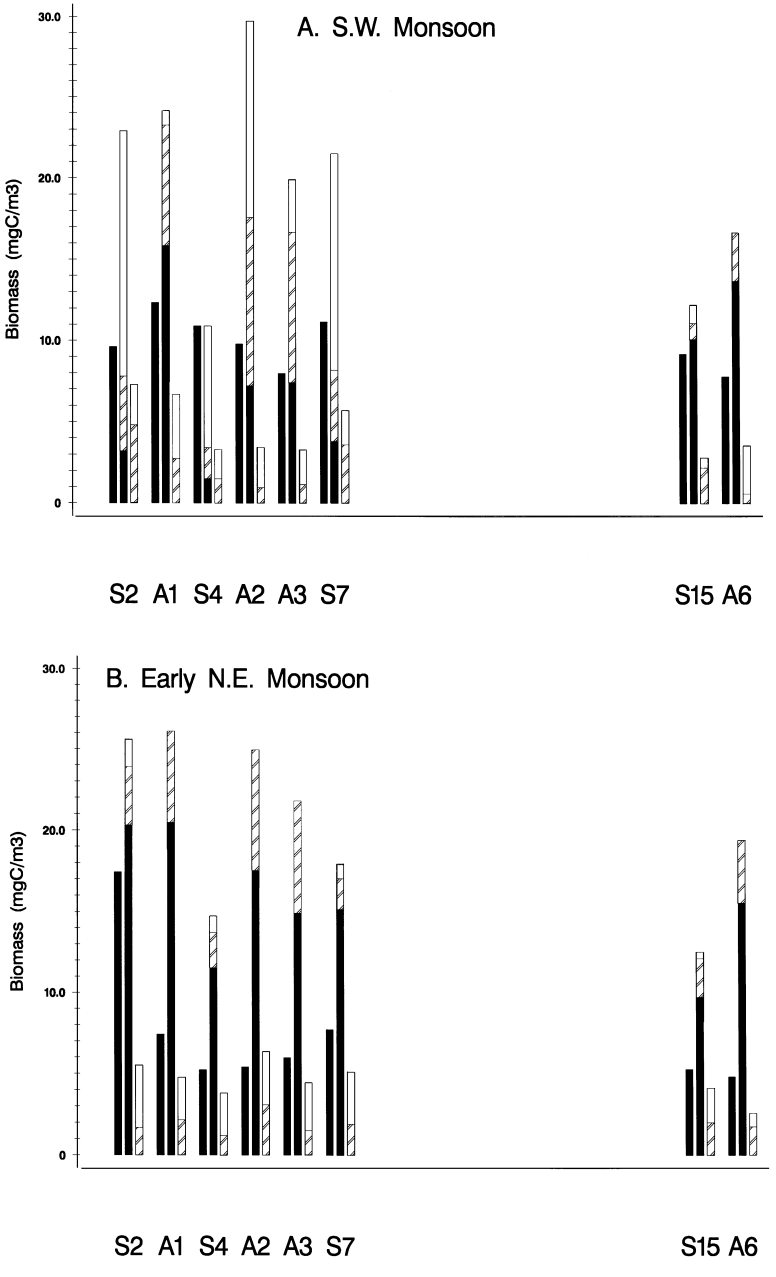

community have been published as separate reports (heterotrophic bacteria: Pomroy and Joint, 1999; phytoplankton: Tarran et al., 1999; zooplankton: Selfox et al., 1999; and pigments: Barlow et al., 1999). Differing conversion factors for cell carbon (e.g., 250 fg cell^{-1} for Syn versus our value of 101 or 152 fg cell^{-1}) have been used, so that ARABESQUE estimates for autotrophic picoplankton biomass for similar abundances of cells will differ from ours. Moreover, investigators from the ARABESQUE program have chosen different depth intervals to integrate data over the upper water column (e.g., integration of data to the mixed layer or the 1% light level versus a constant depth), so that a rigorous comparison of data summarized in the above publications is not possible. Nevertheless (after corrections for differing carbon conversions used) there is substantial agreement between the studies (Fig. 6). Comparisons between ARABESQUE and JGOFS stations at similar latitude and distances from shore show comparable ranges of values and similar community structure for both the SW and early NE Monsoon periods. Tarran et al., (1999), however, report considerably higher phytoplankton stocks – up to 9 g C m^{-2} in the upper 80 m during the NW Monsoon – whereas our values never exceed 3 g C m^{-2} (Table 4). These higher values were almost entirely a result of stations sampled closer inshore and slightly north of the JGOFS transect (see Tarran et al., 1999; their Fig. 4). Dense, diatom-dominated blooms also were found at coastal stations in the same region during TN050, but these were not analyzed (Garrison, unpublished observations), and similar observations of dense diatom-dominated populations associated with coastal upwelling filaments also were described by Wood (1999) (also see Brink et al., 1996).

4.4. *Food web structure and carbon flux*

One of the objectives of our study is to relate food web structure to differing carbon-cycling dynamics, and this requires a strategy to recognize and define differing food-web structure. This is not easy to accomplish because, in nature, assemblages may appear as a continuum of successional changes over time or across an environmental gradient. Analysis of the individual components of the food web showed relatively few distinct and statistically-significant patterns over season or over the region of the US JGOFS study area (see Table 5). Using the similarity among stations

Fig. 6. Comparison of US JGOFS data (August–December, 1995) with ARABESQUE reports (August–December, 1994) at comparable stations in the northern Arabian Sea. ARABESQUE station A6 was the same location as JGOFS S15. A3 is the same location as S7. ARABESQE stations A1 and A2 were slightly northeast of JGOFS stations S2 and S1 (see Burkill, 1999 and our Fig. 1). JGOFS data are from our Table 5, but recombined and shown as an average biomass (μg C l^{-1}) from data integrated to 100 m. ARABESQUE Hbac data are from Pomroy and Joint, 1999 (their Table 1; average Hbac biomass above 1% light levels). Phytoplankton data were taken from Tarran et al., 1999 (their Fig. 4; values recalculated from depth-integrated data over the upper 80 meters). Biomass for Syn was recalculated using our conversion of 101 fg cell^{-1} (see Table 2) as compared with 250 fg cell^{-1} used by Tarran et al. (1999). Zooplankton data from Stelfox et al., 1999 (their Figs. 3 and 9; data recalculated from values integrated over the mixed layer). (A) SW Monsoon, (B) Early NE Monsoon. Legend is the same as that used for Fig. 2.

(PSI: Fig. 4) as a guide for aggregating station data (and making some adjustments so that our observations could be related to other data, such as sediment traps and larger zooplankton abundance), however, we have identified differing food web configurations (Fig. 7). As previously discussed, these groupings correspond to differences in water mass characteristics (Fig. 6), suggesting that the percentage similarity analysis may be a robust method to objectively define community structure. Although many of the fluxes indicated in Fig. 7 will be determined from studies still being analyzed and the details of carbon cycling will be considered more completely as part of the synthesis and modeling phase of the US JGOFS studies (e.g., Sarmiento and Armstrong, 1997), some relationships between community structure and food web dynamics are apparent.

Assemblages present throughout the study area during the Spring Intermonsoon (TN045: Fig. 7d), the early NE Monsoon (TN054: Fig. 7g), and assemblages at offshore station S15 throughout most of the study (Fig. 7c, f, and h) were markedly dominated by autotrophic picoplankton (Fig. 2), with *Prochlorococcus* often comprising the dominant autotroph (Table 5). Microzooplankton grazing estimates by Landry et al. (1998) and Caron and Dennett (1999) show that grazing rates usually balanced phytoplankton potential growth rates at these stations ($m/\mu_0 = 1$; see Fig. 7). The combination of small primary producers and the ability of the microzooplankton to utilize fully the daily production indicate that most of the carbon fixed will be cycled through the microbial food web. Station S15 also was characterized by generally lower larger zooplankton biomass (Smith et al., 1998b) and very low rates of flux from the upper water column throughout the study (Trap MS5: Honjo et al., 1999).

Although the approximate balance of primary production and microzooplankton grazing indicates the importance of the nano- and microconsumers in carbon cycling, this assemblage may comprise up to three trophic levels (e.g., Reckermann and Veldhuis, 1997; Calbet and Landry, 1999). This complexity allows for considerable variability in the efficiency of carbon cycling. In many of the examples (Fig. 7b–d, f) microheterotrophs appear to be reduced relative to heterotrophic nanoplankton. This observation may be related to the predominance of picoplankton sized prey, which would be appropriate to support small particulate feeders (i.e., a multi-level trophic cascade as described by Reckermann and Veldhuis, 1997). Under other conditions, where there is a wider size spectrum of primary producers, prey availability may be the result of increases in the abundance of grazing microzooplankton (see Garrison et al., 1998; their Figs. 5–7). Alternatively, the relative reduction in microheterotrophs when larger zooplankton are abundant (Fig. 7b, d and e) could result from top-down grazing control (although see Calbet and Landry, 1999).

In contrast to the picoplankton-dominated situations, stations with significant nano- and microplankton biomass (e.g., 7b, e and g) often had microzooplankton grazing/ phytoplankton growth ratios that were < 1. The extremes occurred during the NE (Fig. 7b) and SW Monsoon (Fig. 7e). The unbalanced microzooplankton grazing rates suggest situations where phytoplankton stocks could increase, significant carbon could pass directly from phytoplankton to larger grazing zooplankton, or phytoplankton stocks could sink from the water column ungrazed. The relatively small range of productivity and chlorophyll *a* biomass over the study (Table 1) and the

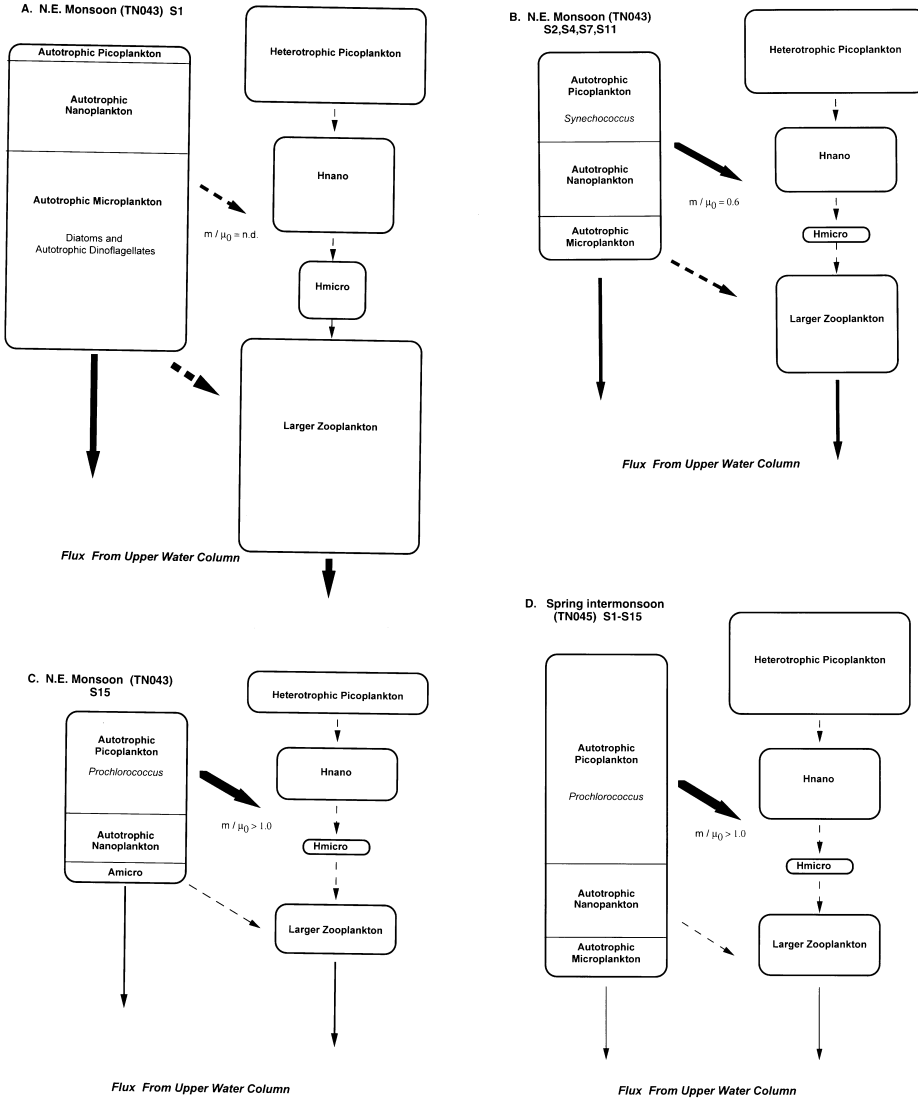

Fig. 7. Conceptual food web structure diagrams showing seasonal and spatial variability. Stations were grouped within cruises based on similarity (see Fig. 5) by single linkage clustering within cruises (data not shown) and watermass properties (Fig. 5 and discussed in text). Relative biomass of food web components is indicated by area of boxes. Zooplankton data are from Roman and Gauzens and Wishner and Gowing (http://www1.whoi.edu/jgofs.html). Microzooplankton rates are shown as the ratio of grazing mortality (m) to phytoplankton growth (μ_0) as determined by dilution grazing measurements (Landry et al., 1998; Caron et al., 1999). In cases where μ_0 was negative in the original data, ratio is shown as > 1.0. Fluxes from the upper water column are indicated as arrows relative to maximum flux estimates (Honjo, unpublished data; see Honjo et al., 1999; and discussed in text). The trap station nearest to the station or group of stations was used as the vertical flux reference. Rates shown as dashed arrows will be determined from modeling studies or from data still being analyzed.

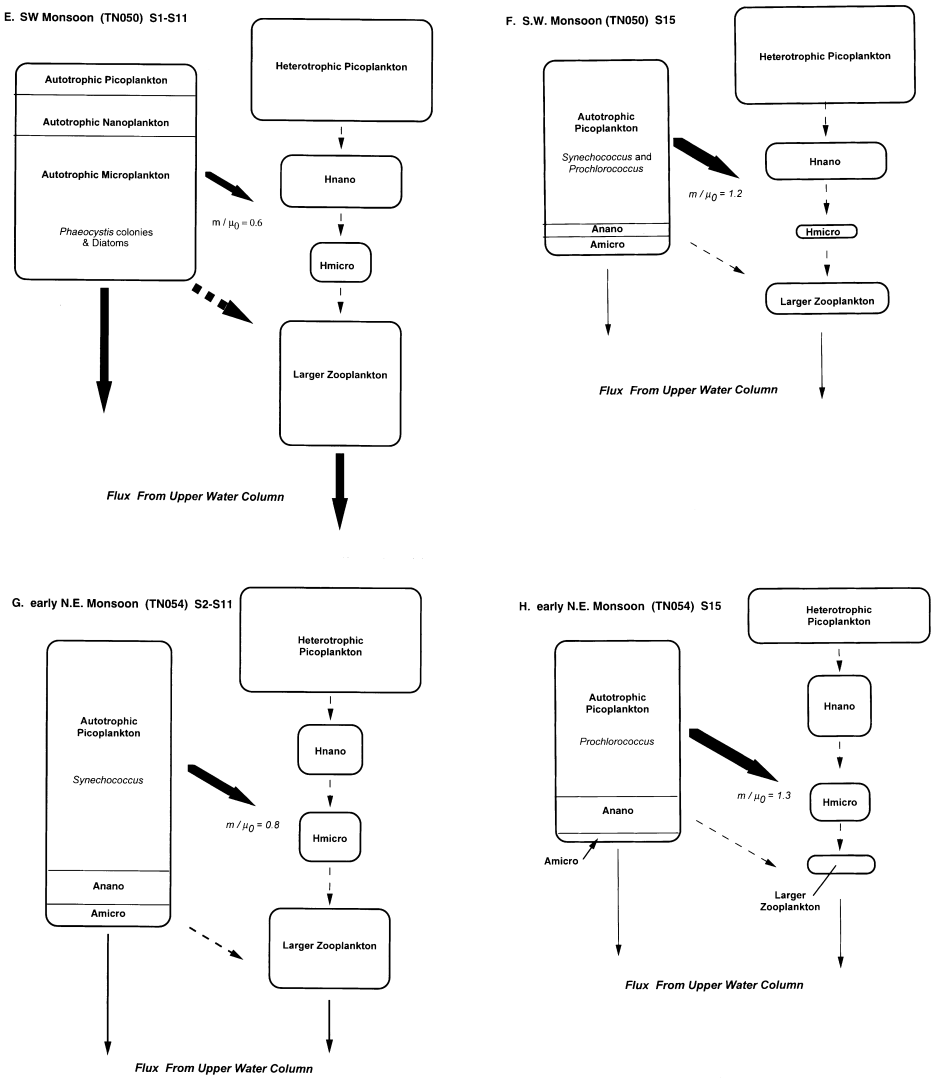

Fig. 7 (*continued*)

lack of statistical significant change in biomass parameters between seasons (and usually among stations within cruises) suggest the latter two possibilities are more important, as does the relative increase in larger phytoplankton that would favor these processes. Smith et al. (1998b) reported that seasonal maxima of mesozooplankton occurred during the during the SW Monsoon at inshore stations and that zooplankton stocks could consume approximately 70% of the daily primary production (Fig. 7e). Significant zooplankton stocks also were present during the NE

Monsoon, and their grazing rates were estimated to remove about 50% of the daily production rate (Fig. 7a and b).

The relationship between food web structure and carbon flux from the surface waters is of particular interest in the context of the JGOFS program. Seasonal variations in the flux from surface waters were dramatic, with most of the mass flux reaching shallow traps during the SW Monsoon (Honjo et al., 1999). Mass flux was higher during both the NE and SW Monsoon seasons in comparison to the intermonsoon periods (Fig. 7), and both were characterized by increases in biogenic silica. The flux patterns differed between the monsoon seasons, with the NE Monsoon characterized by a single modest peak, whereas high fluxes occurred during the SW Monsoon in a series of peaks from approximately mid-July through mid-September. Peaks during the SW Monsoon also differed among the different trap locations with respect to timing, magnitude of the flux, and the composition (e.g., the biogenic silicate content). As discussed previously, mass flux was generally low at offshore station S15 (MS5; Honjo et al., 1999). Flux estimates based on thorium-234 were similar to those based on traps with respect to seasonal and spatial patterns of carbon flux (Buesseler et al., 1999).

The pulses in fluxes of biogenic silicate seem clearly related to diatom blooms. We found diatom-dominated autotrophic assemblages during both the NE and SW Monsoons, but diatoms were more prevalent during the latter with respect to both maximum biomass and spatial extent (Fig. 7a,b vs. e; and see Table 5). During the late SW Monsoon (TN050), diatom-rich populations extended well offshore, apparently associated with mesoscale circulation features linked to upwelling along the Omani coast (see Brink et al., 1996; Garrison et al., 1998; Manghnani et al., 1998; Flagg and Kim, 1998). Our observations in mid-August to mid-September were somewhat after major flux events were recorded in sediment traps (see Honjo et al., 1999), and quantitative data were scarce for the larger phytoplankton during the early part of the SW Monsoon. Wood (1999) reported diatom dominated populations at some nearshore stations in July, and workers on the German JGOFS cruise also reported diatom-rich populations near stations S1, S7, and S11 (K. von Brockel, unpublished observations).

The prevalence of diatoms in the coastal upwelling system of the northern Arabian Sea is not particularly surprising, because these forms are frequently associated with upwelling systems (Dugdale et al., 1995). Based on a model by Young and Kindle (1994), high concentrations of both nitrate and silica in the coastal upwelling waters off the Omani coast and subsequent transport off shore would explain the prevalence of diatoms during the SW Monsoon. Morrison et al. (1998) reported N ($NO_3 + NO_2 + NH_4$) concentrations of $\sim 16\ \mu M$ with corresponding Si concentrations of about 10 μM at station S1 during the late SW Monsoon, consistent with the assumptions of the Young and Kindle model. Diatoms comprised a significant fraction of the phytoplankton biomass at some stations during the NE Monsoon (TN043; see Fig. 7a and Table 5), but the spatial extent of these blooms was restricted, and the flux signal in sediment traps was considerably less than was observed during the SW Monsoon (Honjo et al., 1999). Maximum surface nutrient concentrations during TN043 at all stations in the US JGOFS study area were about 6 μM N, with

a N : Si ratio of about 1.6. At these low nutrient concentrations, there is little potential for diatom biomass accumulation before populations would become silicate-limited (Morrison et al., 1998). It seems reasonable to suggest that diatom blooms during the NE monsoon may be limited to periods (or regions) when mixing transports deep water into the euphotic zone (nitrogen concentrations in deep water are similar through the year, ranging from around 20–22 μM, with cruise average N : Si ratios ranging from 1.6 to 1.9). Recent studies in the upwelling system off the California coast, however, also have shown the potential for iron-limited diatom growth to control bloom distribution patterns (Hutchins et al., 1998). As suggested by Codispoti (1991), Fe limitation is unlikely during the SW Monsoon because of the atmospheric transport of dust trace, but this source of trace metals is considerably less during the NE Monsoon. If true, diatom blooms during the NE Monsoon may be restricted to coastal stations where Fe sources are available from shelf sediments (e.g., see Johnson et al., 1997).

Although the development of conditions that favor diatom blooms seems to be the prerequisite for the strong seasonal signal of biogenic silica flux from surface waters in the Northern Arabian Sea during the SW Monsoon, other factors may also be important. Diatom blooms in other locations have been observed to form aggregates (marine snow) and sink ungrazed (Alldredge and Silver, 1988; Alldredge and Gotschalk, 1989; Wassmann, 1998). The co-occurrence of diatom and *Phaeocystis* blooms during the SW Monsoon (Garrison et al., 1998; Wood, 1999) also could enhance sinking as a result of the mucilaginous material (TEP) produced by *Phaeocystis* (Passow and Wassmann, 1994; Hong et al., 1997; Wassmann, 1998). Seasonal increases in grazing mesozooplankton may also enhance flux. Smith et al. (1998b) reported that zooplankton at coastal stations (inshore from approximately S7) during the SW Monsoon may consume 70% of the daily primary productivity, and they predicted that flux of fecal pellets should be high. Both fecal pellets as well as intact diatom cells are present in sediment trap material from the SW Monsoon (Gowing, unpublished observations), but work on determining the relative importance of sinking diatom populations versus fecal pellets has just begun.

Flux from the upper water column can be directly related to productivity. However, because there was a relatively small seasonal range of primary productivity (Table 1 and see Barber et al., 2000) and considerable variability in the loss of material from the upper water column (Buesseler et al., 1998; Honjo et al., 1999), differences in primary production cannot account for the variability in flux. Similarly, although Smith et al. (1998b) reported that zooplankton grazers reached their maximum during the SW Monsoon, they found that the grazer biomass and potential grazing rates, at least at nearshore stations, were high throughout much of the year. Therefore, it seems unlikely that variability in zooplankton grazing alone would explain the marked variability in downward flux of carbon. In contrast, the correlation between food web make-up, in particular the increasing size fractions associated with diatom blooms during the SW Monsoon is striking and suggests that the primary determinant of flux in this system is likely to be the abundance of diatoms (e.g., Boyd and Newton, 1999).

Although the present synthesis is preliminary and based largely on biomass data, the findings suggest that the results of large scale studies, such as the US JGOFS

Arabian Sea, will be useful in refining conceptual ideas about carbon cycling dynamics and providing data for evaluating biogeochemical models. For example, picoplankton dominated food webs, as we described for some regions of the US JGOFS study area, characterize large areas of the oligotrophic ocean regions (e.g., Buck et al., 1996). Although it has been suggested that these systems may be dominated by heterotrophs (i.e., with biomass of heterotrophic bacteria exceeding primary producers: Fuhrman et al., 1989), this is not supported by the observations of Buck et al. (1996) or the present study (Figs. 2 and 7, and Tables 4 and 5). Reports of the so-called "inverted biomass" relationship (at least in low-latitude oligotrophic oceans) could be explained by using inappropriate carbon biomass estimates for oceanic bacteria (e.g., Fukuda et al., 1998), counting *Prochlorococcus* as Hbac (Geider, 1997), or both. Similarly, the association of high seasonal flux from the upper water column in association with diatom blooms may be examples supporting the role of silica (Dugdale et al., 1995) or iron in controlling biogeochemical processes through their effect on diatom growth (Johnson et al., 1997; Hutchins et al., 1998). Alternatively, the temporal or spatial separation of phytoplankton blooms and zooplankton grazers in a hydrographically dynamic environment such as the northern Arabian Sea also would lead to predictions of increased flux with phytoplankton cells sinking ungrazed (e.g., Legendre and Rassoulzadegan, 1996). The US JOGOFS data base is sufficiently comprehensive that subsequent synthesis and modeling efforts (Sarmiento and Armstrong, 1997) should allow evaluation among competitive conceptual models as well as provide additional insight into the carbon cycling processes during the US JGOFS Arabian Sea Study.

Acknowledgements

We thank the crew of the R.V. *Thomas G. Thompson* for support during the field program. We also thank US JGOFS colleagues, R. Barber, B. Bidigare, L. Codispoti, W. Gardner, A. Gauzens, J. Gunderson, M. Latasa, J. Marra, J. Morrison, M. Roman and K. Wishner for supporting data. We thank Helen Quinby, Flynn Cunningham, Matthew Church and Gary Schultz for technical assistance with bacterioplankton sampling and microscopy; J. Constantinou and H. Nolla for help with sample collection and FCM. Two anonymous reviewers made valuable suggestions to improve the manuscript. This study was supported by the Division of Ocean Sciences, National Science Foundation with a grant to D.L. Garrison and M.M. Gowing (OCE93-10634), M.R. Landry and L. Campbell (OCE93-11246 and OCE96-12509), R.J. Olson (OCE93-11113), H.W. Ducklow (OCE96-00601), and D.A. Caron (OCE93-106931).

References

Alldredge, A.L., Gotschalk, C., 1989. Direct observations of the mass flocculation of diatom blooms: characteristics, settling velocities and formation of diatom aggregates. Deep-Sea Research 36, 159–171.

Alldredge, A.L., Silver, M.W., 1988. Characteristics, dynamics and significance of marine snow. Progress in Oceanography 20, 41–82.

Armstrong, R.A., 1994. Grazing limitation and nutrient limitation in marine ecosystems: steady state solutions of an ecosystem model with multiple food chains. Limnology and Oceanography 39, 597–608.

Azam, F., Fenchel, T., Field, J.G., Gray, J.S., Meyer–Reil, L.A., Thingstad, F., 1983. The ecological role of water-column microbes in the sea. Marine Ecology Progress Series 10, 257–263.

Baldwin, W.W., Bankston, P.W., 1988. Measurement of live bacteria by Normarski interference microscopy and stereologic methods as tested with macroscopic rod-shaped models. Applied Environmental Microbiology 54, 105–109.

Barber, R.T., Marra, J., Bidigare, R.R., Codispoti, L.A., Halpern, D., Smith, S.L., 2000. Primary productivity responses to the Arabian Sea Monsoons. Deep-Sea Research II, in press.

Barlow, R.G., Mantoura, R.F.C., Cummings, D.G., 1999. Monsoonal influence on the distribution of phytoplankton pigments in the Arabian Sea. Deep-Sea Research II 46, 677–699.

Bockstahler, K.R., Coats, D.W., 1993. Spatial and temporal aspects of mixotrophy in Chesapeake Bay dinoflagellates. Journal of Eukaryotic Microbiology 40, 49–60.

Booth, B.C., 1993. Estimating cell concentrations and biomass of autotrophic plankton using microscopy. In: Kemp, P.F., Sherr, B.F., Sherr, E.B., Cole, J.J. (Eds.), Handbook of Methods in Aquatic Microbial Ecology. Lewis Publishers, Boca Raton, pp. 327–338.

Boyd, P.W., Newton, P.P., 1999. Does planktonic community structure determine downward particulate carbon flux in different oceanic provinces? Deep-Sea Research I 46, 63–91.

Brown, S., Landry, M., Barber, R., Campbell, L., Garrison, D., Gowing, M., 1999. Picophytoplankton dynamics and production in the Arabian Sea during the 1995 Southwest Monsoon. Deep-Sea Research II 46, 1745–1768.

Brink, K.H., Jones, B.H., Lee, C.M., Wood, M., 1996. A cool filament off Oman, June 1995: origins and fates of its water. EOS Transactions, AGU 77 (46), F382.

Buck, K.R., Chavez, F.P., Campbell, L., 1996. Basin-wide distributions of living carbon components and the inverted trophic pyramid of the central gyre of the North Atlantic Ocean, summer 1993. Aquatic Microbial Ecology 10, 283–298.

Buesseler, K., Ball, L., Andrews, J., Benitez–Nelson, C. Belastock, R., Chai, F., Chao, Y., 1998. Upper ocean export of particulate organic carbon in the Arabian Sea derived from thorium-234. Deep-Sea Research II 45, 2461–2487.

Burkill, P.H., 1999. ARABESQUE: an overview. Deep-Sea Research II 46, 529–547.

Button, D.K., Robison, B.R., 1993. Use of high-resolution cytometry to determine the activity and distribution of aquatic bacteria. In: Kemp, P.F., Sherr, B.F., Sherr, E.B., Cole, J.J. (Eds.), Handbook of Methods in Aquatic Microbial Ecology. Lewis Publishers, Boca Raton, pp. 163–174.

Calbet, A., Landry, M.R., 1999. Mesoplankton influences on the microbial food web: Direct and indirect trophic interactions in the oligotrophic open ocean. Limnology and Oceanography 44, 1370–1380.

Campbell, L., Nolla, H.A., Vaulot, D., 1994. The importance of *Prochlorococcus* to community structure in the central North Pacific Ocean. Limnology and Oceanography 39, 954–961.

Campbell, L., Landry, M.R., Constantinou, J., Nolla, H.A., Liu, H., Brown, S.L., Caron, D.A., 1998. Response of microbial community structure to environmental forcing in the Arabian Sea. Deep-Sea Research II 45, 2310–2326.

Capriulo, G.M., 1990. Feeding-related ecology of marine protozoa. In: Capriulo, G.M. (Ed.), Ecology of Marine Protozoa. Oxford University Press, New York, pp. 186–250.

Caron, D.A., 1983. Technique for enumeration of heterotrophic and phototrophic nanoplankton, using epifluoresence microscopy, and comparison with other procedures. Applied and Environmental Microbiology 46, 491–498.

Caron, D.A., Goldman, J.C., Fenchel, T., 1990. Protozoan respiration and metabolism. In: Capriulo, G.M. (Ed.), Ecology of Marine Protozoa. Oxford University Press, New York, pp. 307–322.

Caron, D.A., Swanberg, N.R., 1990. The ecology of planktonic sarcodines. Reviews in Aquatic Sciences 3, 147–180.

Caron, D.A., 1991. Evolving role of protozoa in aquatic nutrient cycles. In: Reid, P.C., Turley, C.M., Burkill, P.H., (Eds.), Protozoa and Their Role in Marine Processes. NATO ASI Series, Vol. G25. Springer, Berlin, pp. 387–415.

Caron, D.A., Dam, H.G., Kremer, P., Lessard, E.J., Madin, L.P., Malone, T.C., Napp, J.M., Peel, E.R., Roman, M.R., Youngbluth, M.J., 1995. The contribution of microorganisms to particular carbon and nitrogen in surface waters of the Sargasso Sea near Bermuda. Deep-Sea Research 42, 943–972.

Caron, D., Dennett, M., 1999. Phytoplankton Growth and Mortality during the 1995 Northeast Monsoon and Spring Intermonsoon in the Arabian Sea. Deep-Sea Research II 46, 1665–1690.

Chisholm, S.W., Olson, R.J., Zettler, E.R., Goericke, R., Waterbury, J.B., Welschmeyer, N.A., 1988. A novel free-living prochlorophyte abundant in the oceanic euphotic zone. Nature 334, 340–343.

Choi, J.W., Stoecker, D.E., 1989. Effects of fixation on cell volume of marine planktonic protozoa. Applied and Environmental Microbiology 55, 1761–1765.

Codispoti, L.A., 1991. Primary production and carbon and nitrogen cycling in the Arabian Sea. In: Smith et al. (Eds.), US Joint Global Ocean Flux Study, Arabian Sea Process Study. U.S. JGOFS Planning Report 13, Woods Hole Oceanographic Inst., MA, pp. 75–85.

Coleman, A.W., 1980. Enhanced staining of bacteria in natural environments by fluorochrome staining of DNA. Limnology and Oceanography 25, 948–951.

Dennett, M.R., Caron, D.A., Murzov, S.A., Polikarpov, I.G., Gavrilova, N.A., Georgieva, L.W., Kuzmenko, L.V., 1999. Abundance and Biomass of Nano- and Microplankton Assemblages during the 1995 Northeast Monsoon and Spring Intermonsoon in the Arabian Sea. Deep-Sea Research II 46, 1691–1717.

Ducklow, H.W., Smith, D.C., Campbell, L., Landry, M.R., Quinby, H.L., Steward, G., Azam, F., 2000a. Heterotrophic bacterioplankton distributions in the Arabian Sea: basinwide response to high primary productivity. Deep-Sea Research II, in press.

Ducklow, H.W., Campbell, L., Landry, M.R., Quinby, H.L., Smith, D.C., Steward, G., Azam, F., 2000b. Heterotrophic bacterioplankton distributions in the Arabian Sea: a geographical test of the DOC storage hypothesis. Deep-Sea Research II, in press.

Dugdale, R.C., Wilkerson, F.P., Minas, H.J., 1995. The role of a silicate pump in driving new production. Deep-Sea Research I 42, 697–719.

Eppley, R.W., Reid, F.M.H., Strickland, J.D.H., 1970. Estimates of phytoplankton crop size, growth rate, and primary production. In: Strickland, J.D.H., (Ed.), The ecology of the plankton off La Jolla California in the period April through September, 1967. vol. 17. Bulletin of Scripps Institution of Oceanography, La Jolla, CA, pp. 33–42.

Field, J.G., Clarke, K.R., Warwick, R.M., 1982. A practical strategy for analyzing multisipecies distribution patterns. Marine Ecology Progress Series 8, 37–52.

Flagg, C.N., Kim, H.-S., 1998. Upper ocean currents in the northern Arabian Sea from shipboard ADCP measurements collected during the 1994–1996 US JGOFS and ONR program. Deep-Sea Research II 45, 1917–1960.

Fuhrman, J.A., Sleeter, T.D., Carlson, C.A., Proctor, L.M., 1989. Dominance of bacterial biomass in the Sargasso Sea and its ecological implications. Marine Ecology Progress Series 57, 207–217.

Fuhrman, J.A., McManus, G.B. 1984. Do bacteria-sized marine eukaryotes consume significant bacterial production? Science 224, 1257–1260

Fukuda, R., Ogawa, H., Nagata, T., Koike, I., 1998. Direct determination of carbon and nitrogen contents of natural bacterial assemblages in marine environments. Applied and Environmental Microbiology 64, 3352–3358.

Garrison, D.L., Gowing, M.M., 1993. Microzooplankton. In: Friedmann, E.I., (Ed.), Antarctic Microbiology. Wiley, New York, pp. 123–165.

Garrison, D.L., Gowing, M.M., Hughes, M.P., 1998. Nano- and microplankton in the northern Arabian Sea during the Southwest Monsoon, August–September, 1995: a US JGOFS study. Deep-Sea Research II 45, 2269–2300.

Geider, R., 1987. Light and temperature dependence of the carbon to chlorophyll *a* ratio in microalgae and cyanobacteria: implications for physiological growth of phytoplankton. New Phytology 106, 1–34.

Gifford, D.J., 1991. The protozoan-metazoan trophic link in pelagic ecosystems. Journal of Protozoology 38, 81–86.

Glover, H.E., Cambpell, L., Prezelin, B.B., 1986. Contributions of *Synechococcus* to size fractionated primary production in three water masses in the Northwest Atlantic Ocean. Marine Biology 91, 193–203.

Gowing, M.M., Garrison, D.L., 1992. Abundance and feeding ecology of larger protozooplankton in the ice edge zone of the Weddell and Scotia Seas during the austral winter. Deep-Sea Research 39, 893–919.

Haas, L.W., 1982. Improved epifluorescence microscopy for observing planktonic microorganisms. Annals of the Institute of Oceanography, Paris S58, 261–266.

Hong, Y., Smith Jr., W.O., White, A.-M., 1997. Studies on transparent exopolymer particles (TEP) produced in the Ross Sea (Antarctica) and by *Phaeocystis antarctica* (Prymnesiophyceae). Journal of Phycology 33, 368–376.

Honjo, S., Dymond, J., Prell, W., Manganini, S.J., Ittekkot, V., 1999. Monsoon-controlled export fluxes to the interior of the Arabian Sea: US JGOFS 1994–95 Experiment. Deep-Sea Research II 46, 1859–1902.

Hutchins, D.A., DiTullio, G.R., Zang, Y., Bruland, K.W., 1998. An iron limitation mosaic in the California upwelling regime. Limnology and Oceanography 43, 1037–1054.

Johnson, K.S., Gordon, R.M., Coale, K.H., 1997. What controls dissolved iron concentrations in the world oceans? Marine Chemistry 57, 137–161.

Landry, M.R., Brown, S.L., Campbell, L., Constantinou, J., Liu, H., 1998. Spatial patterns in phytoplankton growth and microzooplankton grazing in the Arabian Sea during monsoon forcing. Deep-Sea Research II 45, 2353–2368.

Latasa, M., Bidigare, R.R., 1997. A comparison of phytoplankton populations of the Arabian Sea during the Spring Intermonsoon and Southwest Monsoon of 1995 as described by HPLC-analyzed pigments. Deep-Sea Research II 45, 2133–2170.

Lee, S., Fuhrman, J.A., 1987. Relationships between biovolume and biomass of naturally derived marine bacterioplankton. Applied and Environmental Microbiology 53, 1298–1303.

Legendre, L., LeFevre, J., 1995. Microbial food webs and the export of biogenic carbon in oceans. Aquatic Microbiology 9, 69–77.

Legendre, L., Rassoulzadegan, F., 1996. Food-web mediated export of biogenic carbon in oceans: hydrodynamic control. Marine Ecology Progress Series 145, 171–193.

Liu, H., Campbell, L., Landry, M.R., Nolla, H.A., Brown, S.L., Constantinou, J., 1998. *Prochlorococcus* and *Synechococcus* growth rates and contributions to production in the Arabian Sea during the 1995 Southwest and Northeast Monsoons. Deep-Sea Research II 45, 2327–2352.

Manghnani, V., Morrison, J.M., Hopkins, T.S., Bohm, E., 1998. Advection of upwelled waters in the form of plumes off Oman during the Southwest Monsoon. Deep-Sea Research II 45, 2027–2052.

Michaels, A.F., Silver, M.W., 1988. Primary production, sinking fluxes, and the microbial food web. Deep-Sea Research 35, 473–490.

Morrison, J., Codispoti, L.A., Gaurin, S., Jones, B., Manghnani, V., Zheng, X., 1998. Seasonal variations of hydrographic and nutrient fields during the US JGOFS Arabian Sea process experiment. Deep-Sea Research II 45, 2053–2101.

Olson, D.B., 1991. Mixed layer dynamics in the Arabian Sea. In: Smith, S., et al., (Ed.), US Joint Global Ocean Flux Study, Arabian Sea Process Study. US JGOFS Planning Report 13. Woods Hole Oceanographic Institute, MA, pp. 49–54.

Olson, R.J., Chisholm, S.W., Zettler, E.R., Altabet, M.A., Dusenberry, J.A., 1990. Spatial and temporal distributions of prochlorophyte picoplankton in the North Atlantic Ocean. Deep-Sea Research I 37, 1033–1051.

Olson, R.J., Zettler, E.R., DuRand, M.D., 1993. Phytoplankton analysis using flow cytometry. In: Kemp, P.F., Sherr, B.F., Sherr, E.B., Cole, J.J. (Eds.), Handbook of Methods in Aquatic Microbial Ecology. Lewis Publishers, Boca Raton, pp. 175–186.

Passow, U., Wassmann, P., 1994. On the trophic fate of Phaeocystis pouchetii (hariot): IV. The formation of marine snow by Pouchetii, P. Marine Ecology Progress Series 104, 153–161.

Peinert, R., von Bodungen, B., Smetacek, V.S., 1989. Food web structure and loss rate. In: Berger, W.H., Smetacek, V.S., Wefer, G. (Eds.), Productivity of the Ocean: Present and Past. Wiley, New York, pp. 35–48.

Pomroy, A., Joint, I., 1999. Bacterioplankton activity in surface waters of the Arabian Sea during and after the 1994 SW Monsoon. Deep-Sea Research II 46, 767–794.

Porter, K.G., Sherr, E.B., Sherr, B.F., Pace, M., Sanders, W., 1985. Protozoa in planktonic food webs. Journal of Protozoology 32, 409–415.

Porter, K.G., 1988. Phagotrophic phytoflagellates in microbial food webs. Hydrobiologia 159, 89–97.

Putt, M., Stoecker, D.K., 1989. An experimentally determined carbon:volume ratio for marine Oligotrichous ciliates from estuaries and coastal waters. Limnology and Oceanography 34, 1097–1103.

Putt, M., 1990. Abundance, chlorophyll content and photosynthetic rates of ciliates in the Nordic seas during summer. Deep-Sea Research 37, 1713–1731.

Riemann, L., Steward, G.F., Fandino, L.B., Smith, D.C., Campbell, L., Landry, M.R., Azam, F., 1999. Bacterial community composition during two consecutive NE Monsoon periods in the Arabian Sea studied by Denaturing Gradient Gel Electrophoresis (DGGE) of rRNA genes. Deep-Sea Research II 46, 1791–1811.

Ryther, J.H., 1969. Photosynthesis and fish production in the sea. The production of organic matter and its conversion into higher forms of life vary throughout the world's ocean. Science 166, 72–76.

Sanders, R.W., Porter, K.G., 1988. Phagotrophic phytoflagellates. Advances in Microbial Ecology 10, 167–192.

Sarmiento, J.L., Armstrong, R.A., 1997. US JGOFS Synthesis and Modeling Project Implementation Plan. US JGOFS Planning and Coordination Office, Woods Hole Oceanographic Institution.

SAS Institute Inc., 1989. SAS/STAT Users Guide, Version 6, 4th Edition, Vol. 2, SAS Institute Inc, Cary, NC.

Sherr, B.F., Sherr, E.B., 1984. Role of heterotrophic protists in carbon and energy flow in aquatic ecosystems. In: Klug, M.J., Reddy, C.A. (Eds.), Current Perspectives in Microbial Ecology. American Society for Microbiology, Washington, DC, pp. 412–423.

Sherr, E.B., Caron, D.A., Sherr, B.F., 1993. Staining of heterotrophic protists for visualization via epifluoresence microscopy. In: Kemp, P.F., Sherr, B.F., Sherr, E.B., Cole, J.J. (Eds.), Handbook of Methods in Aquatic Microbial Ecology. Lewis Publishers, Boca Raton, pp. 213–227.

Shalapyonok, A., Olson, R.J., Shalapyonok, L.S., 2000. Arabian sea phytoplankton during the Southwest and Northeast Monsoons 1995: composition, size structure, and biomass from individual cell properties measured by flow cytometry. Deep-Sea Research II, in press.

Sieburth, J.McN., Smetacek, V., Lenz, J., 1978. Pelagic ecosystem structure: heterotrophic components of the plankton and their relationship to plankton size fractions. Limnology and Oceanography 23, 1256–1263.

Smith, S.L., Banse,K., Cochran, J.K., Codispoti, L.A., Ducklow, H.W., Luther, M.E., Olson, D.B., Peterson, W.T., Prell, W.L., Surgi, N., Swallow, J.C., Wishner, K., 1991. US JGOFS: Arabian Sea Process Study. U.S. JGOFS Planning Report No. 13, Woods Hole Oceanographic Institution, Woods Hole, MA.

Smith, S.L., Codispoti, L.A., Morrison, J.M., Barber, R.T., 1998a. The 1994–1996 Arabian Sea Expedition: an integrated, interdisciplinary investigation of the response of the northwest Indian Ocean to atmospheric forcing. Deep-Sea Research II 45, 1905–1916.

Smith, S.L., Roman, M., Prusova, I., Wishner, K., Gowing, M., Codispoti, L., Barber, R., Marra, J., Flagg, C., 1998b. Seasonal responses of mesozooplankton to monsoonal reversals in the Arabian Sea. Deep-Sea Research II 45, 2369–2404.

Stelfox, C.E., Burkill, P.H., Edwards, E.S., Harris, R.P., Sleigh, M.A., 1999. The structure of zooplankton communities, in the 2 to 200 μm size range, in the Arabian Sea during and after the SW monsoon, 1994. Deep-Sea Research II 46, 815–842.

Stoecker, D.K., Taniguchi, A., Michaels, A.E., 1989. Abundance of autotrophic, mixotrophic and heterotrophic planktonic ciliates in shelf and slope waters. Marine Ecology Progress Series 50, 241–254.

Stoecker, D.K., Capuzzo, J.M., 1990. Predation of protozoa: its importance to zooplankton. Journal of Plankton Research 12, 891–908.

Stoecker, D.K., Gifford, D.J., Putt, M., 1994. Preservation of marine planktonic ciliates: losses and cell shrinkage during fixation. Marine Ecology Progress Series 110, 293–299.

Tarran, G.A., Burkill, P.H., Edwards, E.S., Malcom, E., Woodward, S., 1999. Phytoplankton community structure in the Arabian Sea during and after the SW Monsoon of 1994. Deep-Sea Research II 46, 655–676.

US JGOFS., 1990. US Joint Global Ocean Flux Study, The role ocean biogeochemical cycles in climate change, Long Range Plan. US JGOFS Planning Report Number 11

Verity, P.G., Langdon, C., 1984. Relationships between lorica volume, carbon, nitrogen, and ATP content of tintinnids in Narragansett Bay. Journal of Plankton Research 6, 859–868.

Verity, P.G., Robertson, C.Y., Tronzo, C.R., Andrews, M.G., Nelson, J.R., Sieracki, M.E., 1992. Relationships between cell volume and carbon and nitrogen content of marine photosynthetic nanoplankton. Limnology and Oceanography 36, 729–750.

Verity, P.G., Sieracki, M.E., 1993. Use of color image analysis and epifluorescence microscopy to measure plankton biomass. In: Kemp, P.F., Sherr, B.F., Sherr, E.B., Cole, J.J. (Eds.), Handbook of Methods in Aquatic Microbial Ecology. Lewis Publishers, Boca Raton, pp. 327–338.

Wassmann, P., 1998. Retention versus export food chains: processes controlling sinking losses from marine pelagic systems. Hydorbiologia 363, 29–57.

Wood, A.M., 1999. The Arabian Sea: a natural experiment in phytoplankton biogeography. FY98 Annual Reports, Office of Naval Research, Arlington, VA.

Young, D.K., Kindle, J.C., 1994. Physical processes affecting availability of dissolved silicate for diatom production in the Arabian Sea. Journal of Geophysical Research 99, 22619–22632.